AN INVESTIGATION OF THE EFFECTS OF TURBULENT QUENCHING IN A CAN-TYPE COMBUSTION CHAMBER

A Thesis

Submitted to the Graduate Faculty

of the University of Minnesota

by

Robert S. Hutches

LT, U. S. Navy

In Partial Fulfillment of the Requirements

for the Degree of

Master of Science in Aeronautical Engineering

May 1954

ACKNOWLEDGMENTS

The author wishes to express his appreciation to Dr. Newman A. Hall, Professor Thomas E. Murphy, and Mr. Howard McManus for their interest and advice; to LCDR Winston L. Miller and LT Robert J. Barnes, USN, for their assistance in operating the equipment and reducing data; and to the U. S. Naval Postgraduate School for sponsoring the attendance of the author at the University of Minnesota during this period of graduate study.

TABLE OF CONTENTS

SYMBOLS

A - Area, ft^2.

a - Acoustic velocity, ft/sec.

C_p - Specific heat at constant pressure, BTU/lb.^oR.

D - Diameter, feet.

g - 32.2 ft/sec^2.

k - Constant.

$\dot{m}$ - Mass flow rate, lb/sec.

M - Mach number.

P - Pressure.

Q_L - Lower heating value of fuel, BTU/lb.

R - Gas constant, = 53.34 ft/^oR.

T - Absolute temperature, ^oR.

V - Velocity, ft/sec.

z - Distance from most forward part of the combustion chamber to the centerline of the first quench air port.

γ - Ratio of C_p/C_v.

Δ - Increment or change.

$\Delta P_{2,3}$ - Pressure drop across metering orifice number 2(3).

ρ - Density, lb/ft^3.

η - Efficiency.

Subscripts

$()_1$ - Ambient air.

$()_2$ - Air upstream of main air supply metering orifice.

$()_3$ - Air upstream of vaporizer tube air supply metering orifice.

$()_a$ - Air.

$()_e$ - Exit Cross-Section.

$()_f$ - Fuel.

$()_i$ - Stream tube in exit cross-section.

$()_m$ - Mixture or combustion products.

$()_s$ - Static or Stream values.

$()_t$ - Total or Stagnation values.

$()_{th}$ - Theoretical.

Superscripts

$()^{1,2,etc.}$ - Refer to numbered references in BIBLIOGRAPHY.

SUMMARY

Secondary air injection orifices in an experimental can-type combustion chamber using a vaporizer tube for fuel injection are modified to produce turbulent mixing of the excess air with the combustion products. The results of this investigation are compared with those of a previous project[6] and the following results are noted:

1. Burner thermal efficiences are very slightly reduced.
2. Mixing is thorough, as determined by flame patterns and temperature data.
3. Even temperature and velocity profiles are obtained at the exit cross-section of the combustion chamber.
4. This type of quenching would permit shortening of a 20-inch combustion chamber by at least 2-inches, or 10%.
5. Total pressure losses were doubled, increasing from an average value of 5.6% to 11.3% of the inlet total pressure.

INTRODUCTION

The trend toward the replacement of the piston-engine by turbo-jet and turbo-prop power plants in all phases of high-speed and long-range aircraft has placed renewed emphasis on the investigation and development of the constant-pressure, continuous-flow combustion chamber. Weight and space limitations on aircraft components are equally applicable to the jet engine and its component parts. Operating requirements for a gas turbine power plant demand smooth, dependable long-life operation over a wide range of altitude, engine and aircraft speeds, and periods of acceleration and deceleration. Further design requirements are high heat release per unit volume of combustion chamber, with high combustion efficiency and minimum pressure loss.

Considerable investigation has been done on the chemistry of combustion, propagation of flame fronts, and associated phenomena. Unfortunately this work is not completely applicable to the type of combustion which occurs in the combustion-chamber of a gas-turbine power plant. Here, the flame front actually consists of numerous small individual flame fronts. This situation does not lend itself to easy analysis. Therefore, construction and final configuration of combustion chambers in gas-turbines have been largely a matter of experimentation and testing.

Mass and heat transfers in the combustion process involve four steps: formation of the combustible mixture, ignition or

start of combustion, flame movement or propagation of combustion, and final mixing of the combustion products with excess air.[1]

Some factors affecting the formation of a combustible mixture are here listed. The Bureau of Standards has determined that combustion efficiency of various fuels in moving air increases with an increase in fuel volatility.[2] The rate of evaporation of a droplet of volatile fuel is proportional to the vapor pressure of the fuel, the absolute temperature, and the air turbulence, and is inversely proportional to the molecular weight of the fuel.[3] The air requirements for combustion are proportional to the molecular weight of the fuel, and the time required to form a combustible mixture of air and fuel vapor is directly proportional to the fuel droplet size and is inversely proportional to the relative velocity between the droplet and the air.[4]

Ignition and propagation of combustion might be considered together as a chemical reaction between air and fuel vapor. The combustion process consists of the breaking-down of the complex fuel hydrocarbons into lower molecular weight oxides. During these chain reactions, chain carriers are formed and heat is liberated to further the reaction until combustion is complete. While the rate of these reactions is dependent on many factors, it has been determined that reaction rates are proportional to the absolute temperatures at which they occur and are inversely proportional to the molecular weight of the fuel.[13]

From the above statements it is seen that a vaporizer tube operating with a low molecular weight, highly volatile fuel in turbulent air should be an optimum method of introducing fuel into a combustion chamber. Barnes[6] and Miller[5] have conducted investigations using a vaporizer tube in an experimental combustion chamber, and report high thermal efficiencies as compared to a spray nozzle type fuel injection system.[7]

The final mixing of the combustion products with excess air occurs in the so-called secondary air zone, the airflow having been divided into two main portions. The primary air passes through the primary zone, encompassing steps 1, 2, and 3 above. The secondary air by-passes the primary zone and is injected downstream, cooling the products of combustion to obtain a combustion chamber exit temperature profile in which temperature should not vary more than 5 per cent from its average value, and in which the maximum temperature does not exceed approximately 1700°F.[1]

This secondary air must be injected at high velocities, of the order of 200-300 feet per second, as compared with 15-50 feet per second in the primary zone.[8] The high velocity is needed to obtain penetration of the secondary air into the primary combustion products in a very short period of time, since the space and weight limitations on a jet engine limit the length of the combustor. If thorough mixing is to occur, the order of turbulence must be high. Therefore, not only must high-velocity

streams be used, but they must also be injected in such a manner as to "stir" the mixture thoroughly before it passes downstream to the turbine. Insufficient mixing may allow stratification of the layers of hot gases, possibly even resulting in a tongue of flame impinging on the turbine blades.

Combustion efficiency will decrease, however, if the secondary air is introduced so far upstream that chilling of the products of combustion occurs before the chemical reactions have been completed. Further, a high turbulence level results in a large friction pressure drop through the combustion chamber. Since friction pressure losses are normally of the order of twice the momentum pressure losses due to heating,[1] the friction pressure losses greatly influence the efficiency of the gas-turbine cycle.

Thus the design of a combustion chamber requires, among other things, a delicate balance in the design of the secondary air system. A compromise among burner length, combustion efficiency, pressure losses, and combustion chamber exit (turbine inlet) temperature profile must be made in the design of the secondary air system. At this writing there is no data available to the designer which will insure that if secondary air is admitted in a prescribed pattern that an acceptable combustion chamber will result. This paper will attempt to contribute some data for this design problem, by determining the effect of a controlled, reproducible turbulent air pattern on the factors mentioned in the preceding paragraphs.

EQUIPMENT AND EXPERIMENTAL TECHNIQUE

EQUIPMENT

The combustion chamber used in this experiment was designed and constructed by Janssen.[9] The chamber is shown in Figs. 1, 2 and 14. Air was admitted through 48 ducts, the flow through which was controllable by a damper plate in conjunction with a metering orifice in each duct. The burner was rectangular in cross section, being approximately 2 inches wide, 5 inches high and 20 inches long. The front portion was a semi-circular arc, of radius 2.5 inches, as viewed from the side.

The main air supply consisted of a centrifugal compressor driven by a 165 horsepower Lycoming air-cooled gasoline engine. The air was ducted through a 6-inch pipe to a Y-type manifold where the flow was divided and routed to the lower and upper halves of the burner.

The vaporizer tube for fuel injection was constructed of 5/8-inch outside diameter seamless stainless steel tubing as shown in Fig. 5. The dimensions of the tube and its location in the combustion chamber were determined by Miller[5] and are shown in Fig. 6.

The air through the vaporizer tube was obtained from a high-pressure (100 psig) air line, throttled through a control valve to a 2-inch pipe connected to that portion of the vaporizer

tube outside the combustion chamber.[5,6]

The original secondary air injection orifices in the combustion chamber were modified by inserting steel strips in the original slots to establish a high turbulence level in the quench air zone. This modification is sketched in Fig. 7 and shown in Figs. 8 and 9.

The liquid fuels were pumped to the vaporizer tube by a Vickers constant displacement pump. Fuel flow rate was controlled by a hand-operated external by-pass system. A 1/8-inch needle-valve was installed in the fuel line in order to obtain steady fuel flow at a pressure of 15 psig.

INSTRUMENTATION

The manometer system of Janssen[9] and Ryberg[7] was changed by replacing the common water-mercury manometer system with one containing a separate water-filled U-tube for each of the 48 ducts and the metering orifices of the main and vaporizer tube air supplies (Fig. 3). The traversing temperature and total pressure probes[7] in the exit section were replaced with a rake[5,6] consisting of seven total pressure tubes and seven chromel-alumel temperature probes equally spaced in the vertical plane of the exit section (See Figs. 10 and 11). Static pressure at the exit was obtained by tapping two holes in the side plate of the exit section, one at one-fourth of the distance down on one side and the other three-fourths of the distance down on the opposite side, joining the two

static pressure lines, and feeding the resultant pressure to the water-filled manometer system. There the static pressure was compared with atmospheric pressure and with the pressure from each of the total pressure tubes of the rake.

The main air and vaporizer tube air flow rates were determined by measuring the upstream static pressure and temperature and the pressure drop in inches of water across a square-edged circular orifice in the respective air supply lines. Mass flow rates were computed in accordance with the procedure outlined in Ref. 10 and are shown in Figs. 12 and 13.

The fuel flow into the combustor was measured by a rotometer type fuel flow meter. The meter was calibrated previously[5,6] and, in addition, thirty-minute runs at the design flow rate were made for each fuel to confirm the accuracy of the calibration runs.

Thirty-nine chromel-alumel thermocouples were located in three horizontal rows in the burner as shown in Figs. 14 and 23 and pictured in Figs. 2, 5, 8, and 9. The emf of the thermocouples was determined by potentiometers which had built-in cold junction compensation for iron-iron constantin thermocouples. Thermocouple conversion curves[9] shown in Fig. 15 were therefore used to correct the observed temperature readings.

Iron-iron constantin thermocouples were used to measure compressor outlet air temperature and vaporizer tube air supply temperature upstream of the respective metering orifices.

EXPERIMENTAL TECHNIQUE

Since the primary purpose of this experiment was to determine the effects of changing the method of introducing the quench air, as many other variables as possible were kept constant. Thus, only in the configuration of the secondary air injection orifices did the runs differ from those of Barnes.[6] Combustion intensity, fuel and air flow rates, vaporizer tube configuration and location, and pressure drops in each of the 48 ducts adhered as closely as possible to these values used by Barnes.[6] In addition, in order to use the same technique for each fuel the runs on a particular fuel were always started with the upstream quench air port at position 20 and the quench air was then moved forward in increments of two stations per run. A period of approximately two minutes was allowed after all settings had been made before any pressure or temperature readings were recorded. This was done in order to allow steady conditions to obtain. All temperature and pressure readings at the exit cross section were read simultaneously and this cycle of readings was repeated at least once each run. Temperature readings of the 39 thermocouples in the burner were taken approximately every other run on each fuel to determine the approximate boundary of the flame pattern and the effectiveness of the secondary air as a quenching medium. Fuel temperature, barometer, and relative humidity readings were taken before each set of runs.

The four fuels used in this project were aviation gasoline, naphtha, kerosene, and a diesel fuel. Fuel specifications are included as Appendix A and distillation curves as Fig. 16. The design flow rate of each fuel was chosen to match that selected by Barnes,[6] which in turn was selected so as to maintain the same combustion intensity (BTU heat release per second per cubic foot of combustion chamber volume) for each fuel. Fuel flowmeter calibration curves indicating these design flow rates are shown in Fig. 17.

The actual operating procedure of setting up and running was identical to that used by Barnes.[6] Operating RPM of the main air supply compressor was necessarily increased approximately 300 RPM over that used by Barnes since the modification of the secondary air injection orifices by the insertion of the metal strips caused a flow restriction in the air supply system. In order to maintain the same mass air flow through the burner it was therefore necessary to operate the compressor at a higher pressure ratio, this higher pressure ratio being obtained by increasing the compressor RPM.

A series of runs consisted of burning one fuel at the design flow rate, commencing with the first upstream quench air port at air Station 20 (See Fig. 14) and moving the block of quench air forward in increments of two stations per run.

The quench air pattern consisted of five ports on top

and the five opposing ports on the bottom of the burner, each such duct having a pressure drop across the metering orifice equal to six-inches of water. The remainder of the secondary air ports were adjusted to 0.1 inches of water pressure drop across each metering orifice. The small flow rate through these latter ducts provided air which served the dual purpose of preventing burning in the ducts and keeping the ducts cleared of unvaporized fuel during those runs where kerosene and diesel fuel were used.

The primary air pattern was that determined by Ryberg[7] and subsequently used by Barnes.[6] All pressure-drop settings were adjusted to give the desired values while combustion was occuring. Typical air patterns are shown in Fig. 23.

Total air flow was maintained as constant as possible by (1) hand operation of the needle-valve controlling the air supply to the vaporizer tube to maintain an air flow rate of 0.0218 pounds per second, and (2) varying compressor RPM to maintain a main air supply flow rate of 0.600 pounds per second. These values approximate the average air flow rates used by Barnes.[6] Inability to maintain these exact values is discussed in the section on Errors.

During the initial kerosene run it was noted that vaporized fuel droplets emerged from cracks around thermocouple insulators. The run was stopped and ceramic cement was applied to the cracks. The next run caused the ceramic to crumble at

several locations due to vibration. Further attempts to reseal these cracks proved just as unsuccessful. The kerosene runs were therefore continued with fuel vapor leaking from the chamber. With the quench air at station 20 very little fuel leakage was apparent, but as the quench air was shifted forward the fuel loss increased until at station 10 a cloud of vapor surrounded the thermocouple side of the burner.

Four attempts were made to run diesel fuel at the design flow rate, but all resulted in rich blow-outs. Combustion could be maintained for only about 30 seconds after the butane (used for starting) was turned off before flame-out occurred. Fuel flow rate was reduced in small increments from the design rate of 0.00517 lb/sec to 0.00221 lb/sec before combustion could be maintained. This inability to burn at or near design flow rate was apparently the result of the cementing of the cracks around the thermocouples mentioned above. Since the amount of fuel leakage was reduced considerably, the entrapped fuel vaporized sufficiently to cause the rich blow-outs. As a result, the runs on diesel fuel are not comparable with those of aviation gas, naphtha, or kerosene, since the combustion intensity was reduced to 43% of the design value.

ESTIMATED ERRORS

All pressure measurements could be read within ± 0.05 inches of water or mercury. Temperatures could be read within 1° of the scale value. It is estimated that fuel flowmeter readings were accurate to within ± 0.025 gallons per hour.

While the average fluctuation of the compressor was ± 5 RPM from the desired value, this produced no noticeable variation in the main air supply readings. The velocity head readings on the rake pitot tubes varied ± 0.10 inches of water, which would produce a maximum variation of two feet per second in velocity determinations at high velocities and low densities. The average rake temperature variation was ± 4°F. between successive readings. The main and secondary air metering orifices were standard orifice meters and should provide air flow readings accurate to within ± 2%.[10] Fuel flow rate did not fluctuate, since any movement of the float was more in the nature of a small vibration than an oscillation.

Considering only aviation gasoline, naphtha and kerosene runs, the BTU input per pound of air was 155 ± 10, and the overall air/fuel ratio was 120.5 ± 7.

Steep temperature and velocity gradients existed with the quench air at stations 18 and 20. The mass flow integration and resultant temperature rise computations are likely to be more in

error at stations 18 and 20 than they are with the quench air at stations 16 and forward.

Efficiencies greater than 100% were encountered on several runs. Two factors contribute to this error:

(1) No horizontal traverses of the exit section were attempted. Thus the measured temperatures at the center of the section were considered to extend the width of the cross-section in the exit-section summation of $\rho_i V_i T_i$. Ryberg[7] on this same equipment made one horizontal traverse per run, and determined that the temperature decreases from the centerline toward the edges. This error leads to efficiences that are too high in every case.

(2) No high-temperature calibration of the exit section thermocouples was made. The rake was checked in boiling water; variation of indicated temperatures on all thermocouples did not exceed 1.5°F. from the average temperature.[5] Since the butt-welded thermocouples were surrounded by ceramic shields, it would have destroyed the thermocouples to have checked them in a molten metal.

The moisture content of the air remained at 51 $\pm$ 8 grains of water per pound of dry air. Since this variation was small, omitting the effect of moisture in efficiency computations lead

to a constant error of approximately 0.7% in the efficiency. This was considered negligible. All computations were therefore based on fuel and dry air as inputs to the combustion chamber.

RESULTS

The purpose of this investigation was to determine (1) a method of introducing secondary air in a combustion chamber in such a manner as to cause definite quenching and (2) the effects of such an air pattern on combustion efficiency, combustor length and combustor exit temperature profile, and combustion chamber pressure losses. Since the method used in this experiment was to be compared with that of a preceding method on the same equipment, it was necessary to adopt the same definitions of "efficency" and "optimum combustor length" as that used by Barnes:[6]

Thermal efficiency as used in this paper is therefore defined as the ratio of the actual temperature rise to the theoretical maximum temperature rise of a given mass of air burning in the combustor with a given mass of fuel. The method of determining thermal efficiency is included as Appendix B. Optimum combustor length is that distance from the most forward point of the combustion chamber downstream to the centerline of the first quench air port at which the thermal efficiency of the cycle is at or very near a maximum.

Plots of thermal efficiency vs. combustor length are shown in Figs. 18, 19, 20, 21, and 22 for the four fuels. Aviation gasoline, of lower molecular weight and higher volatility than naphtha, indicates a slightly higher thermal

efficiency (102.0%) as compared with naphtha (101.5%). Both of these fuels exhibit the same shape curve; that is, constant or slightly increasing efficiency from station 20 to station 12, at which point a rapid fall-off in efficiency is apparent. The exit temperature profiles also are similar, with sharp gradients occurring with the quench air at stations 20 and 18, gradients decreasing as the quench air is moved forward, until an almost even temperature profile is obtained with the quench air at station 14 and forward.

The curve of η vs. combustor length for kerosene indicates a linearly-decreasing efficiency from station 20 forward. This is considered to be due to quenching and to the loss of fuel from around the thermocouples mentioned previously.

From the plots of thermal efficiency vs. combustor length, the optimum combustor length for the various fuels was as follows:

Fuel	Air Station
Aviation gasoline	12
Naphtha	12
Kerosene	20

The outputs of the 39 thermocouples inside the combustion chamber were recorded with the quench air at stations 20, 16, 12 and 10 for each of the four fuels. It was assumed that the minimum temperature for combustion to exist was 1850°R. The

flame patterns for these runs was then estimated. Flame patterns for runs on naphtha are shown in Fig. 23. For the three comparable fuels it was shown that the quench air definitely "chopped off" the flame as it passed between the 3rd and 4th quench air ports. The diesel fuel flame pattern was generally shorter and not as well defined as those of the other fuels.

With regard to combustor exit (turbine inlet) allowable temperature (assumed to be 1700°F. maximum), the temperature readings in the chamber indicated that the combustion chamber could have been physically shortened as indicated below without exceeding the maximum temperature limitation at the exit:

	First Quench Air Port
Naphtha - cut at thermocouple #37	12
Aviation gas " " #37	12
Kerosene " " #26	20

This "shortening" would have been based on the quench air being positioned in accordance with the optimum combustor length as defined previously. The limit of 5% variation from average temperature would not, however, have been satisfied.

The total pressure loss on each run was computed in accordance with the procedure outlined in Appendix C and is plotted in Fig. 24. Points were selected from the raw data of Barnes[6] which were near or on each of his final curves of

efficiency vs. combustor length and the pressure loss was computed in the same manner and is also plotted in Fig. 24 for purposes of comparison. It can be seen that introducing the strips in the injection orifices increased the total pressure loss from an average value of approximately 5.6% to an average value of approximately 11.3%. The momentum pressure losses were very nearly equal, within the limits of accuracy of both investigations (See Appendix C). Therefore, the change in total pressure loss is equal to the increased friction pressure loss due to the modification of the injection orifices and the resultant turbulence in the burner.

Summarizing, the results of this investigation clearly showed that with either aviation gasoline or naphtha as a fuel, quenching was positively effected and completely extinguished the flame between the third and fourth quench air ports. Relatively high efficiences were also attained. The temperature and velocity profiles at the exit of the chamber were acceptable as turbine inlet profiles. Total pressure losses were doubled (increased from 5.6% to 11.3%) due to the highly turbulent flow.

The vaporizer tube was not capable of efficiently handling kerosene as a fuel, and would not even operate with diesel fuel at the design flow rate.

BIBLIOGRAPHY

1. Godsey, F. W., and Young, L. A., Gas Turbines for Aircraft, New York: McGraw-Hill Book Co., Inc., 1949.

2. Olson, L. O., F. W. Ruegg, and F. R. Caldwell, "Combustion in Moving Air," S.A.E. Quarterly Transactions, April, 1949.

3. Clarke, J. S., "Combustion in Aero Gas Turbines," Engineering September 15, 1950, 170:230-232.

4. Elliott, M. A., "Combustion of Diesel Fuel," S.A.E. Quarterly Transactions, Vol. 3, 1949.

5. Miller, W. L., Master of Science Thesis submitted to the University of Minnesota, 1954.

6. Barnes, R. J., Master of Science Thesis submitted to the University of Minnesota, 1954.

7. Ryberg, J. G., Master of Science Thesis submitted to the University of Minnesota, 1953.

8. Vincent, E. T., The Theory and Design of Gas Turbines and Jet Engines, New York: McGraw-Hill Book Co., Inc., 1950.

9. Janssen, J. E., Master of Science Thesis submitted to the University of Minnesota, 1953.

10. Flow Measurement 1949, A.S.M.E. Power Test Codes.

11. Pinkel, I. V., and H. Shames, Analysis of Jet-Propulsion Engine Combustion-Chamber Pressure Losses, NACA TN 1180, Government Printing Office, Washington, D. C., February, 1947.

12. North American Combustion Handbook, The North American Manufacturing Co., Cleveland, Ohio, 1952.

13. Griswold, John, Fuels, Combustion and Furnaces, New York: McGraw-Hill Book Co., Inc., 1946.

14. ASTM Test Code: D86-40.

15. ASTM Test Code: D323-43.

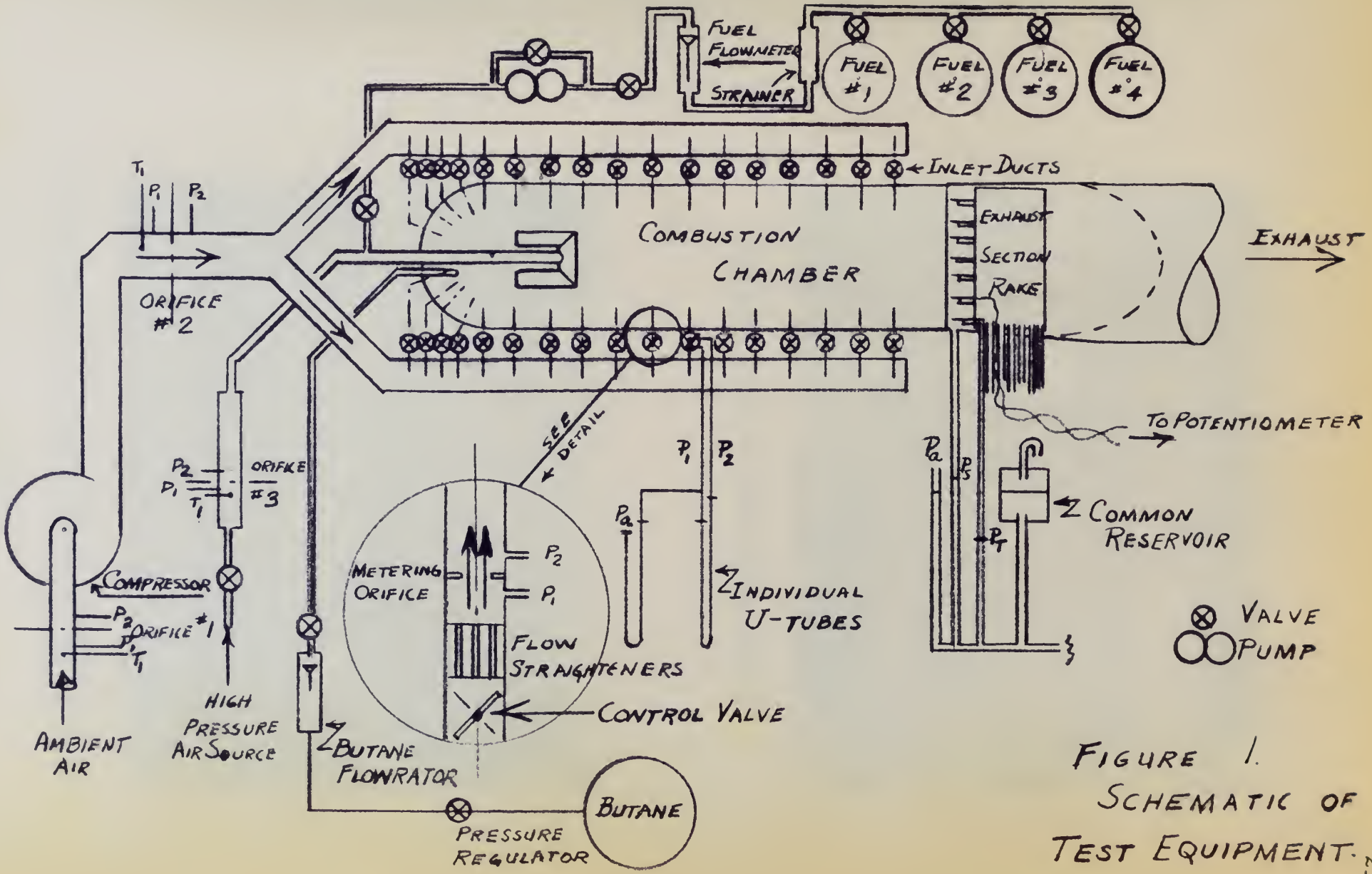

FIGURE 1.
SCHEMATIC OF
TEST EQUIPMENT.

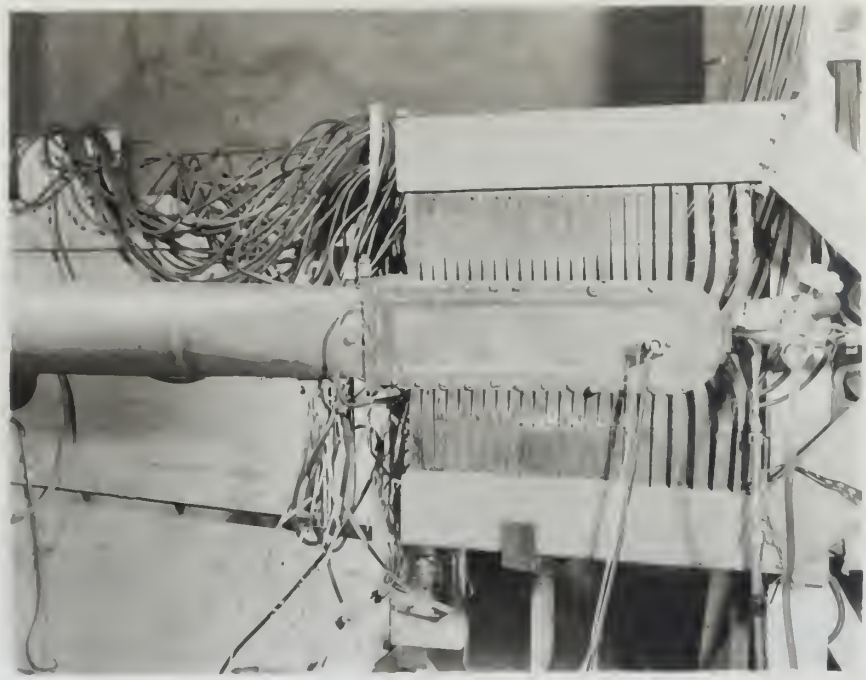

(a) Side View of Combustion Chamber.

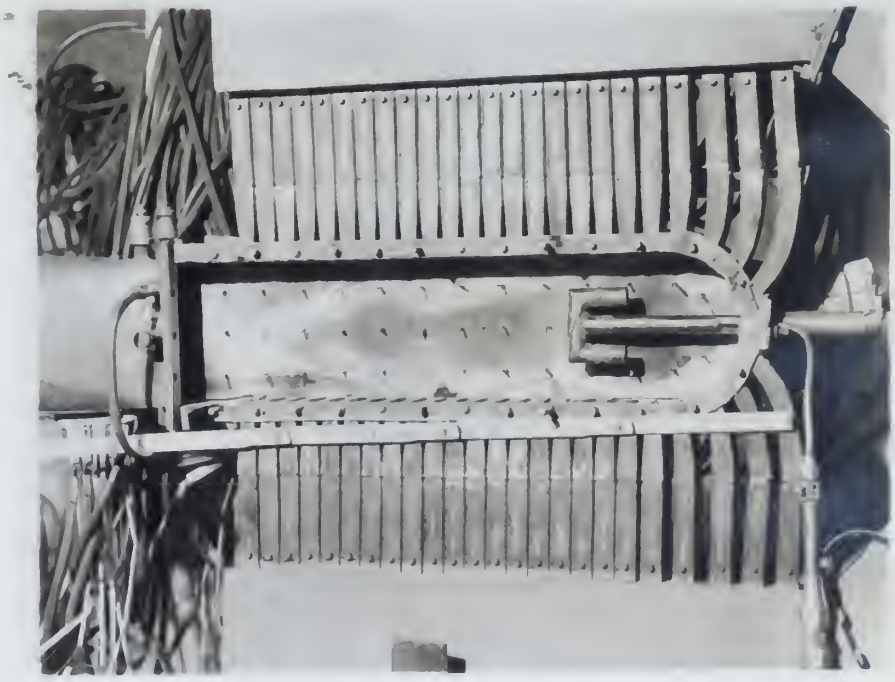

(b) Combustion Chamber With Side Plate Removed.

Figure 2

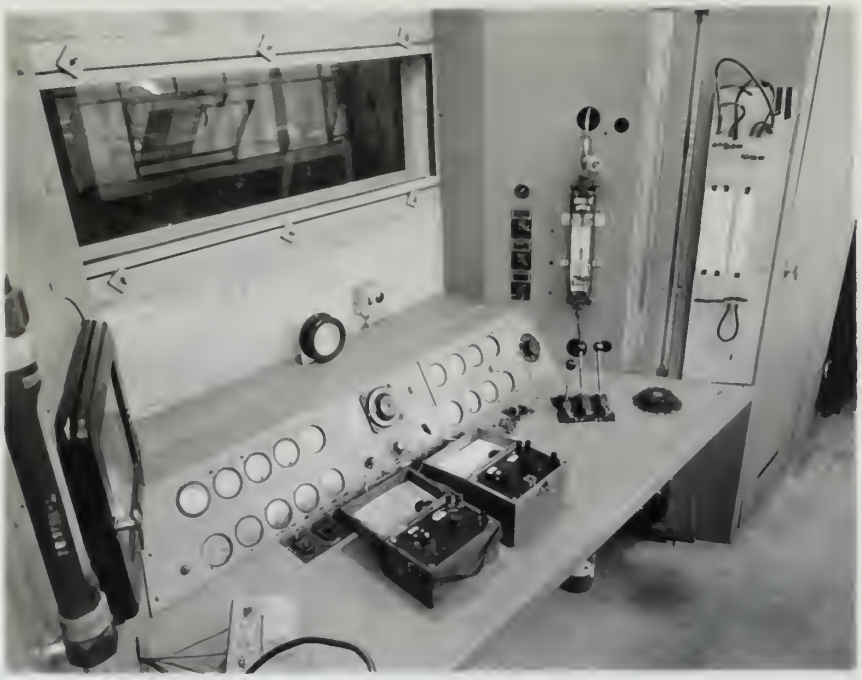

Figure 3 - Test Cell Control Panel.

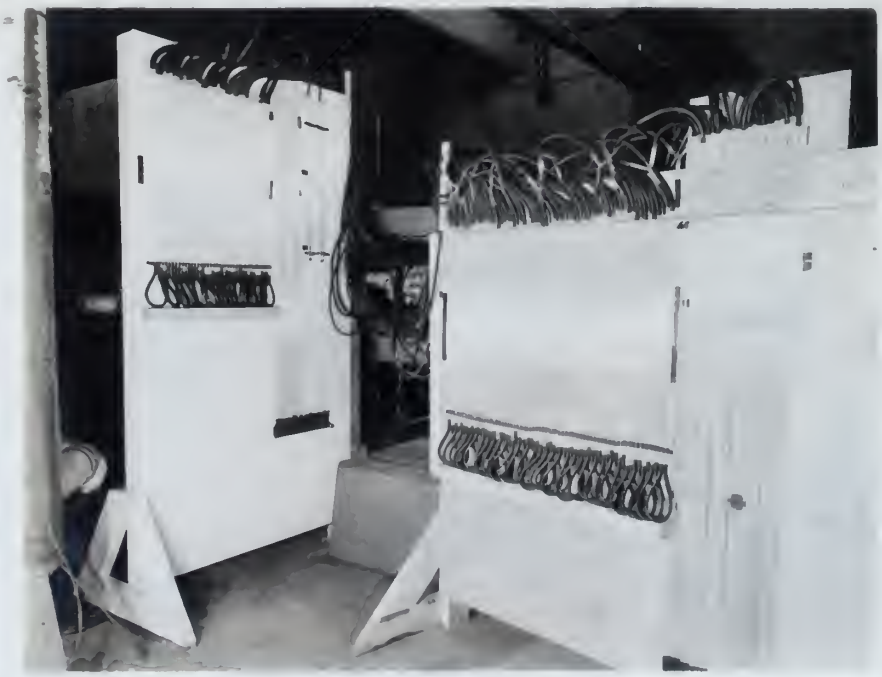

Figure 4 - Manometer System.

(a) Vaporizer Tube.

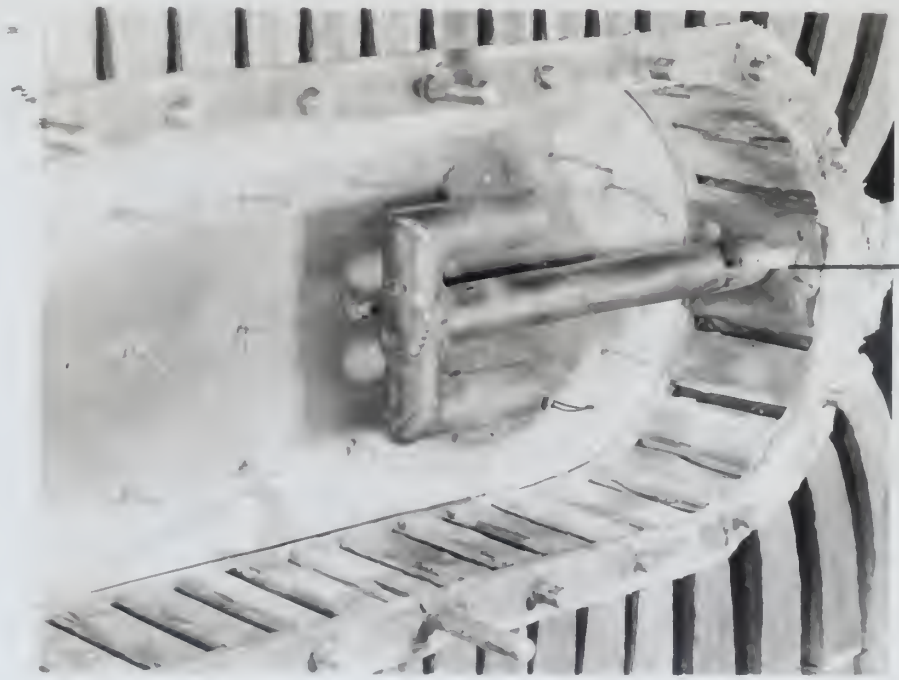

(b) Vaporizer Tube Installed

Figure 5

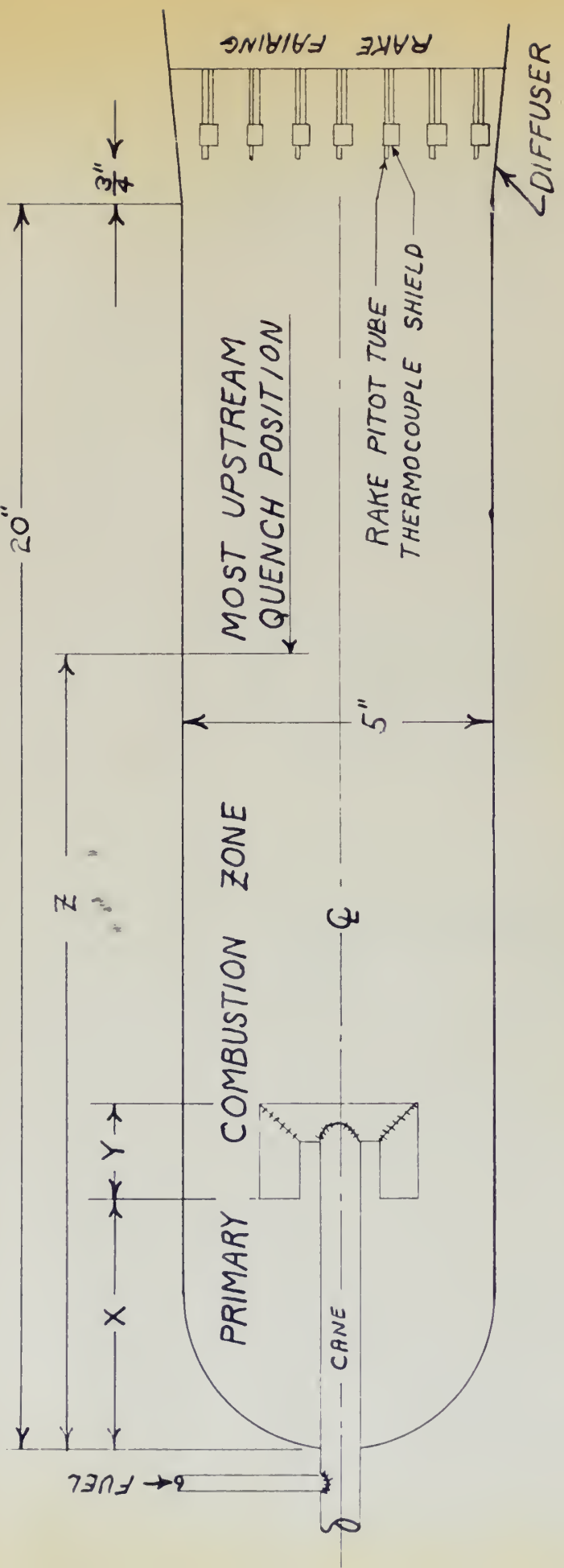

FIG. 6. SIDE ELEVATION OF COMBUSTOR SHOWING CANE AND RAKE LOCATIONS

Figure 8 - Combustion Chamber Showing Lower Injection Orifices as Modified.

Figure 9 - Close-up of Modified Lower Injection Orifices.

Figure 10 - Exit Cross-section Rake, Assembled.

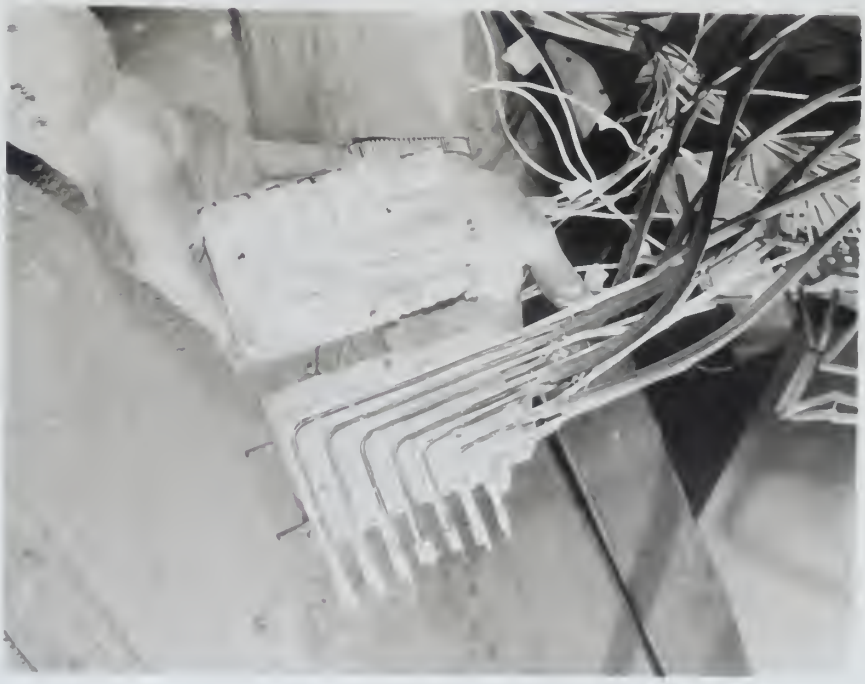

Figure 11 - Exit Cross-section Rake, Showing Construction.

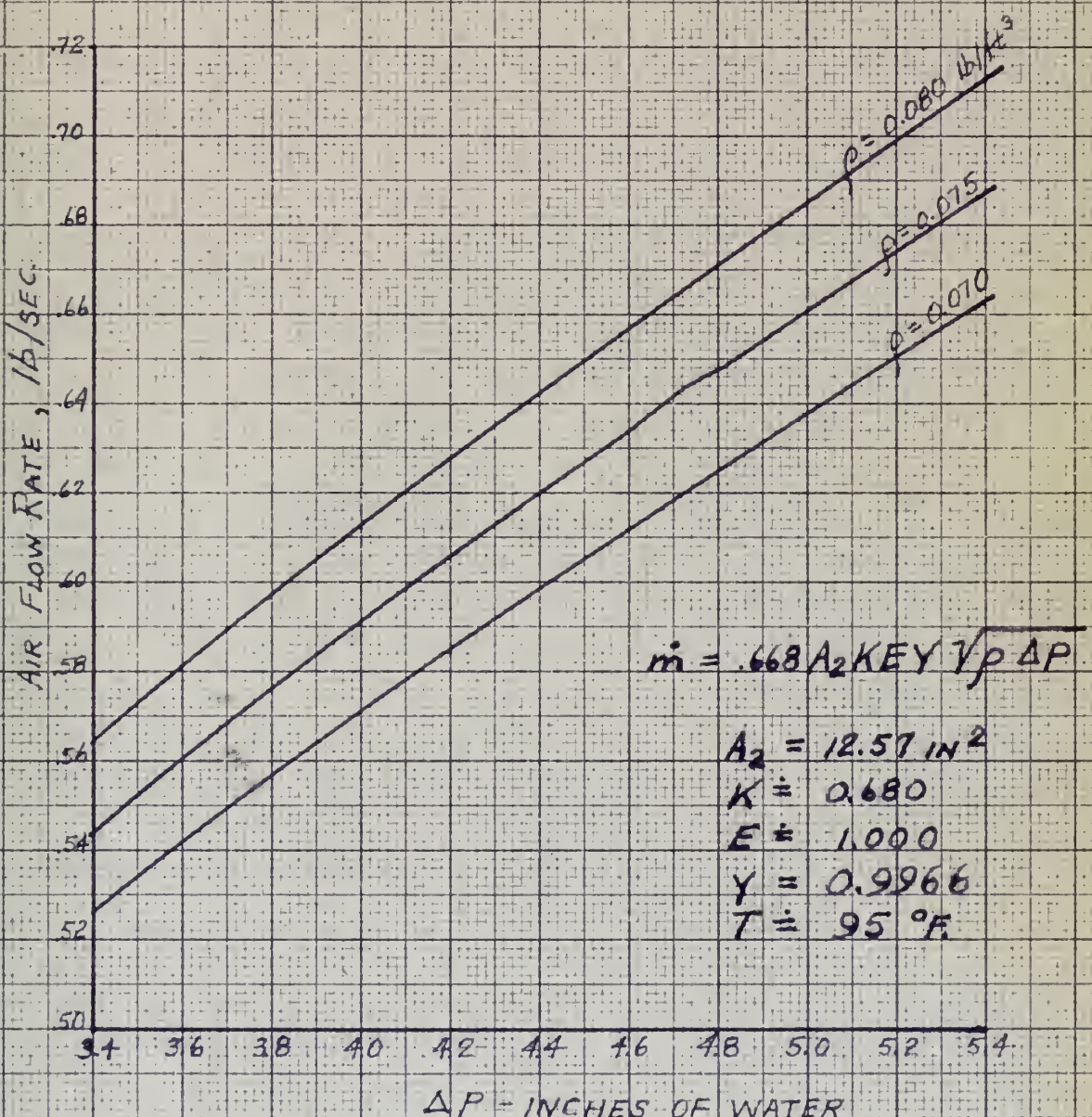

FIGURE 12 - AIR FLOW RATE FOR ORIFICE #2.

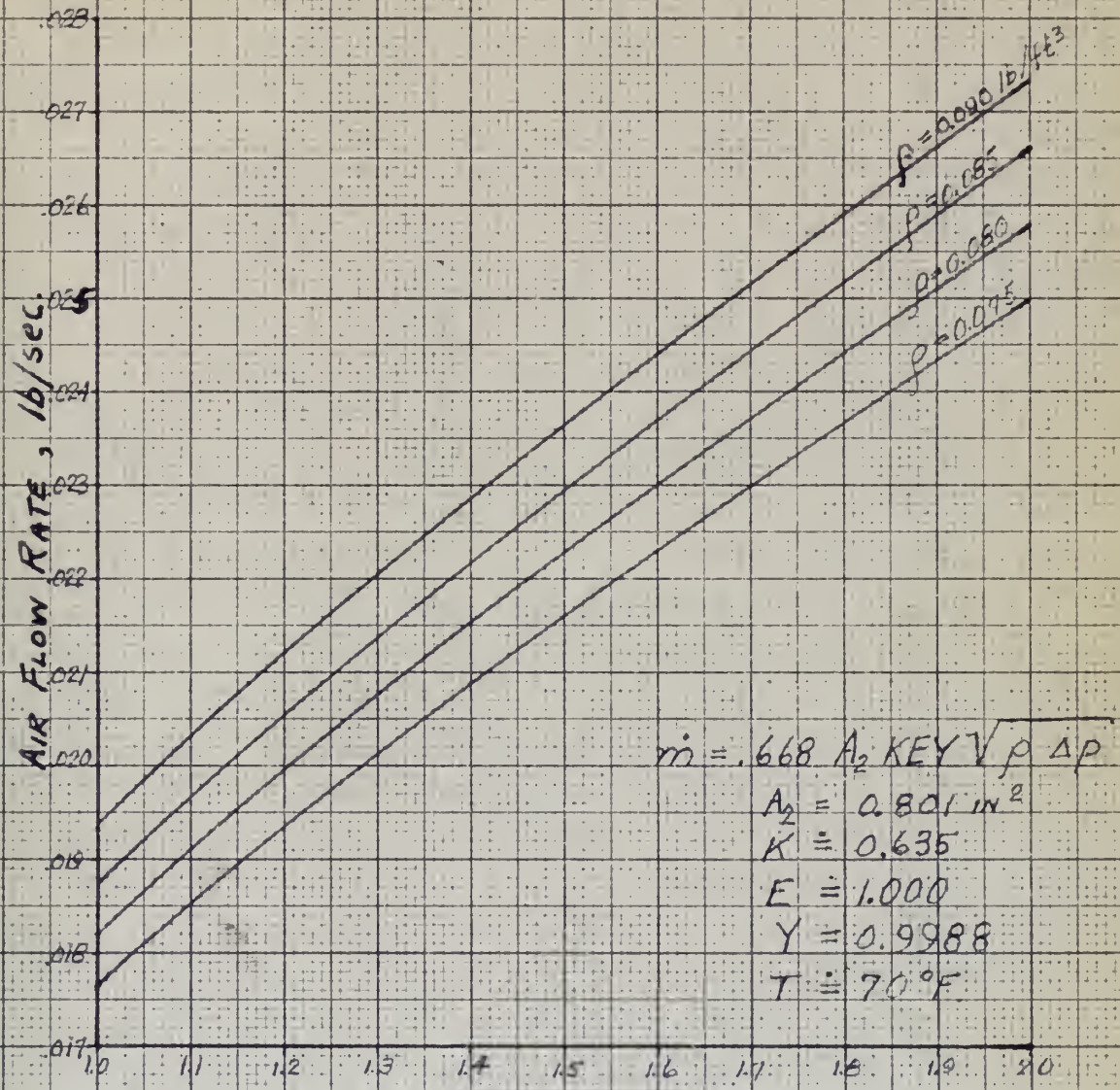

FIGURE 13 - AIR FLOW RATE FOR ORIFICE #3

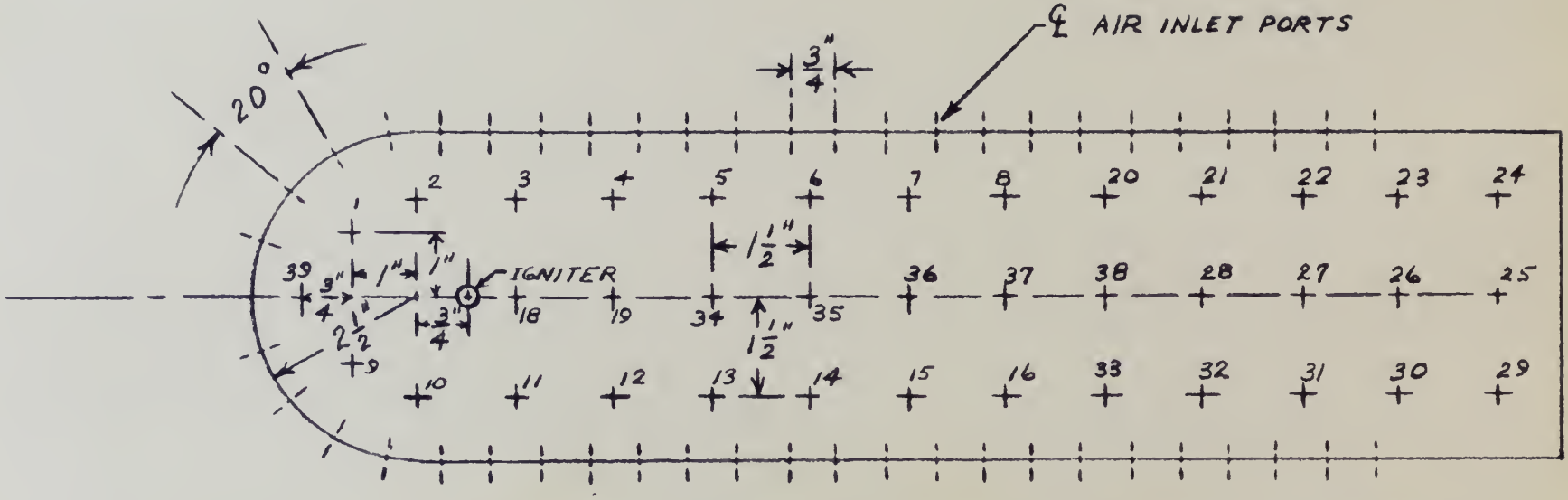

FIGURE 14 - SCALE SCHEMATIC OF COMBUSTION CHAMBER.

SCALE: 1" = 2 2/3".

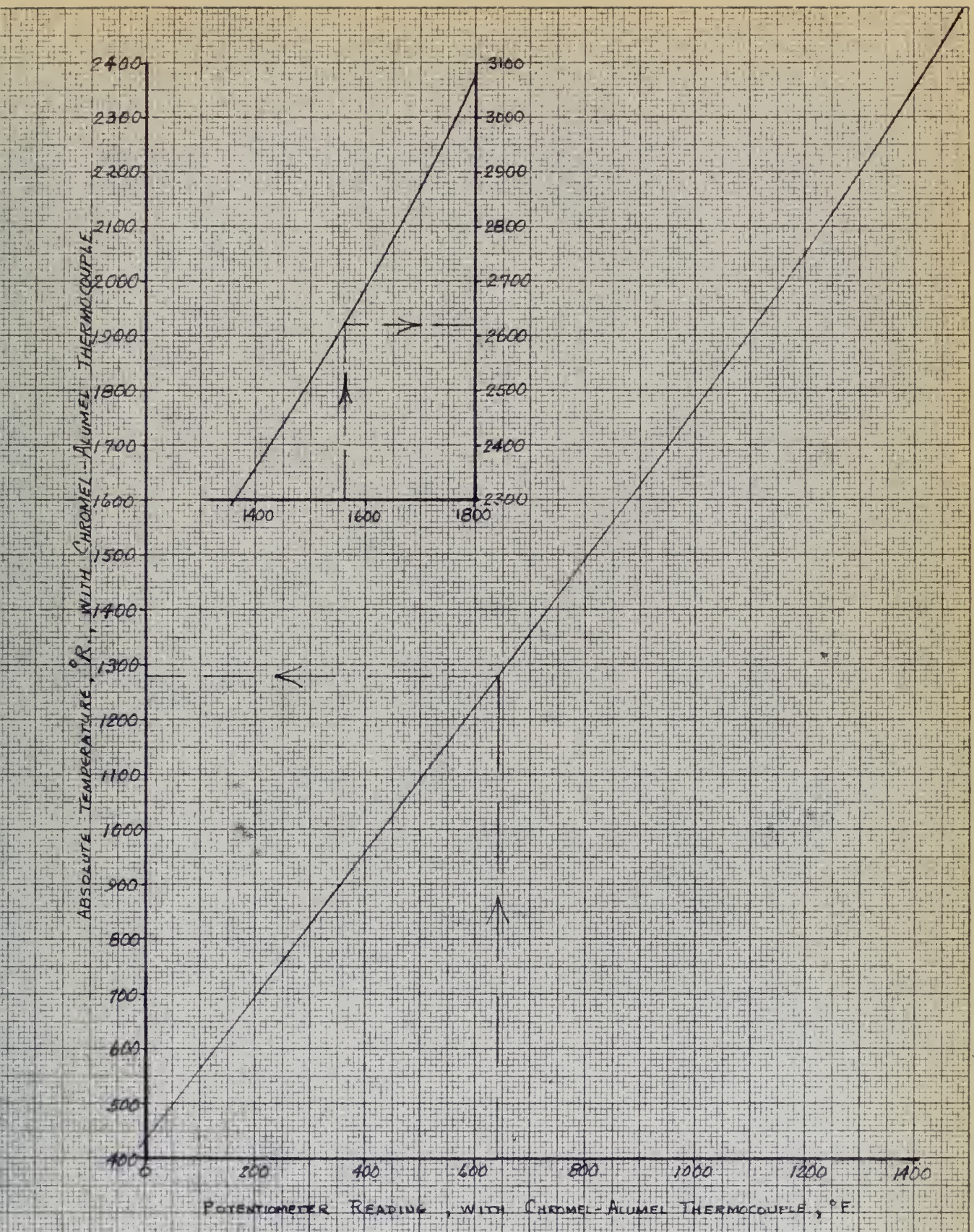

FIGURE 15 - THERMOCOUPLE CONVERSION CURVE.

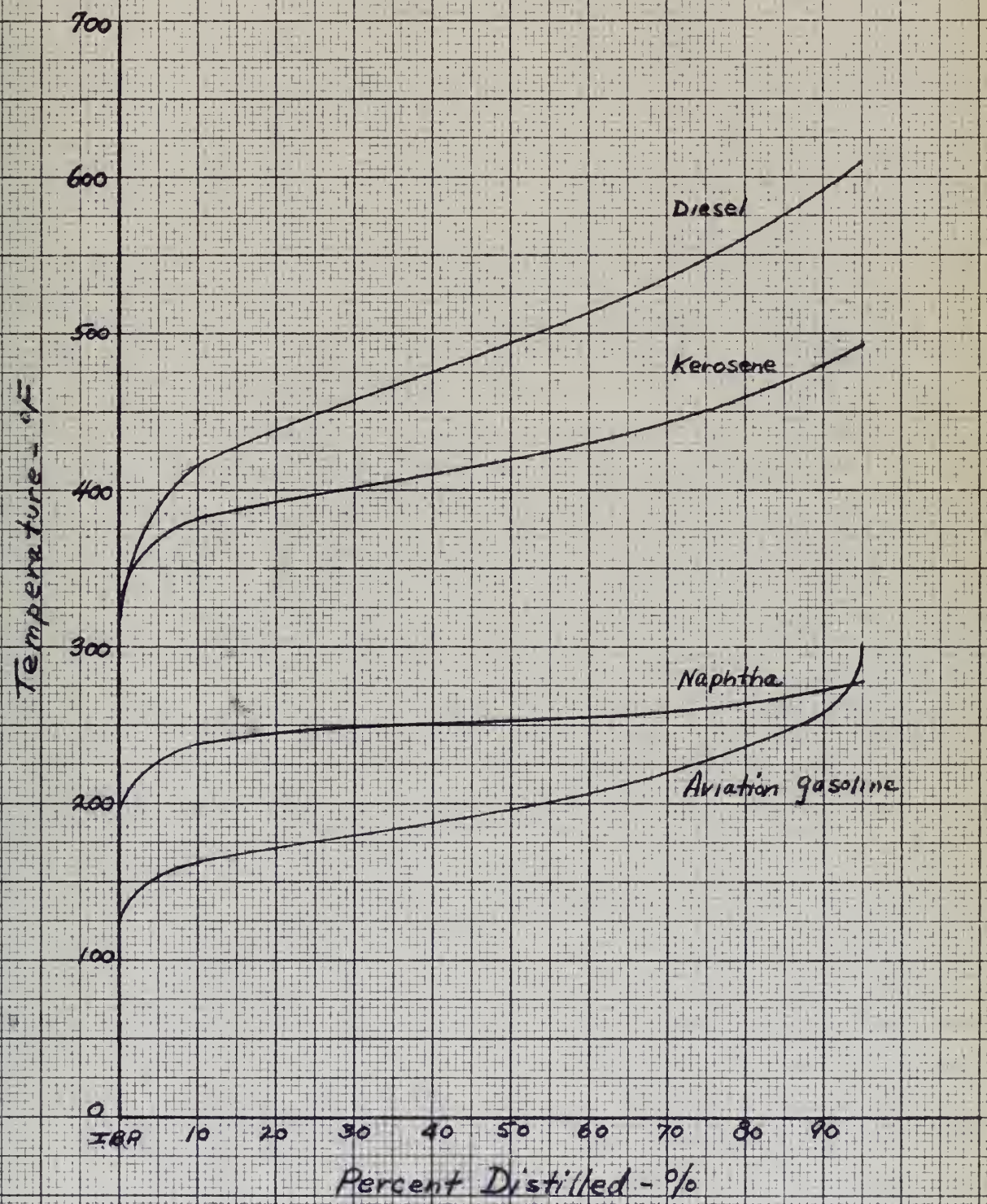

Fig. 16 - ASTM Fuel Distillation

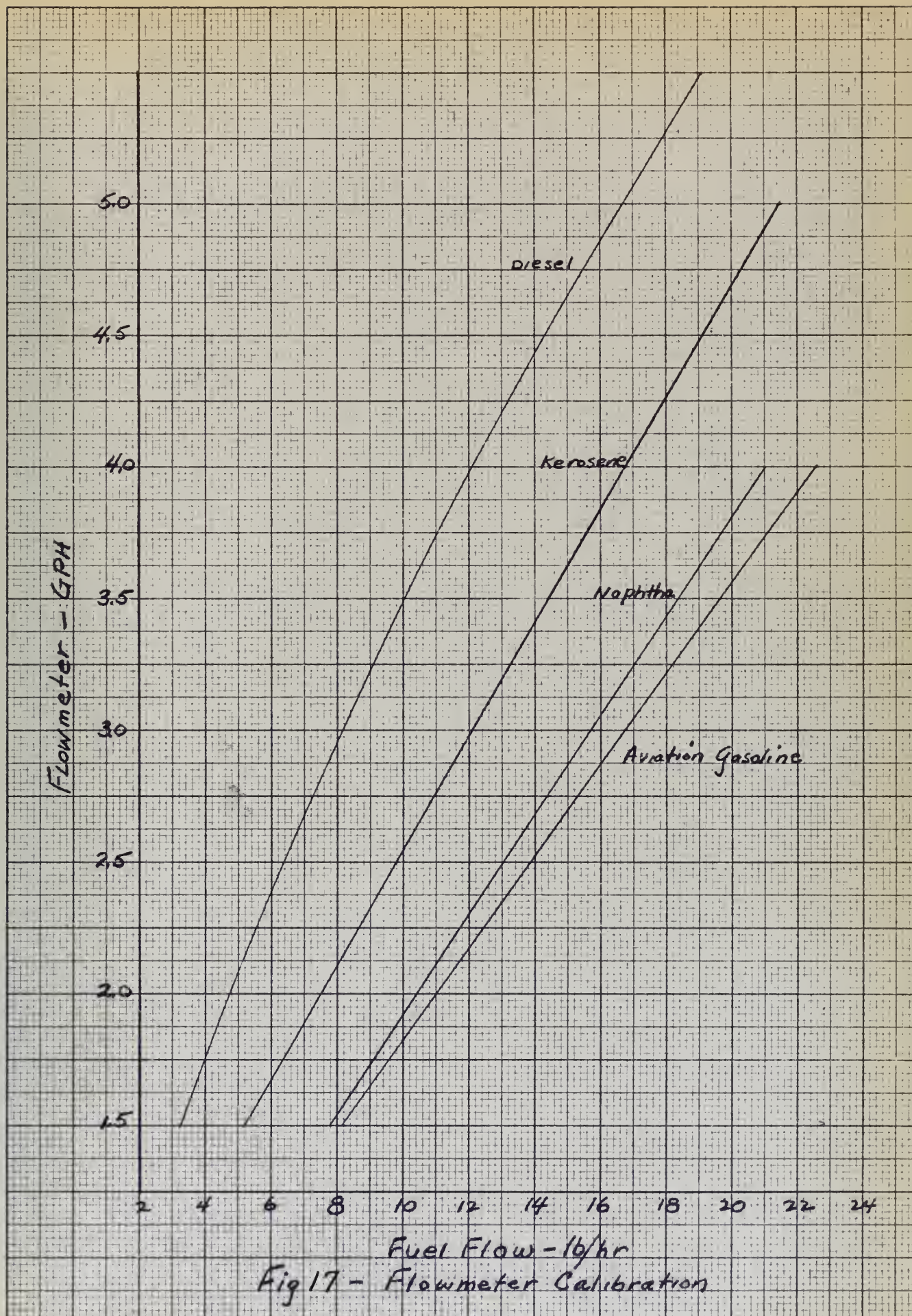

Fig 17 - Flowmeter Calibration

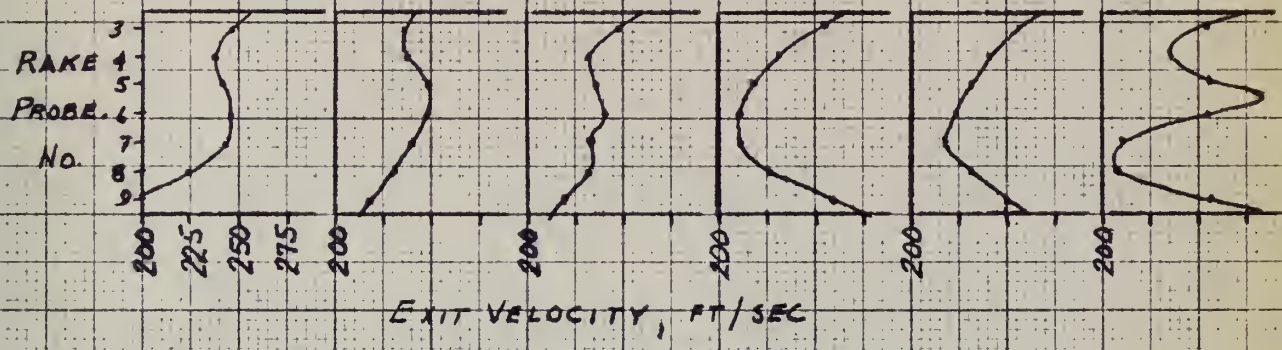

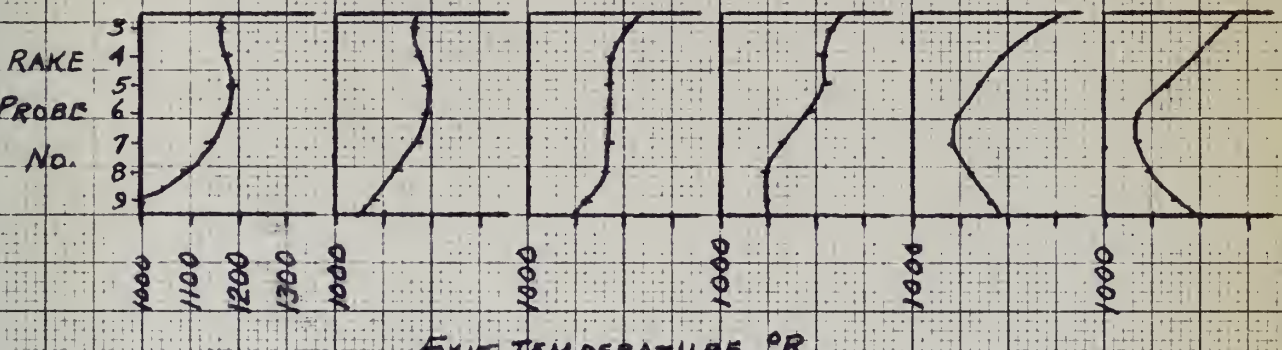

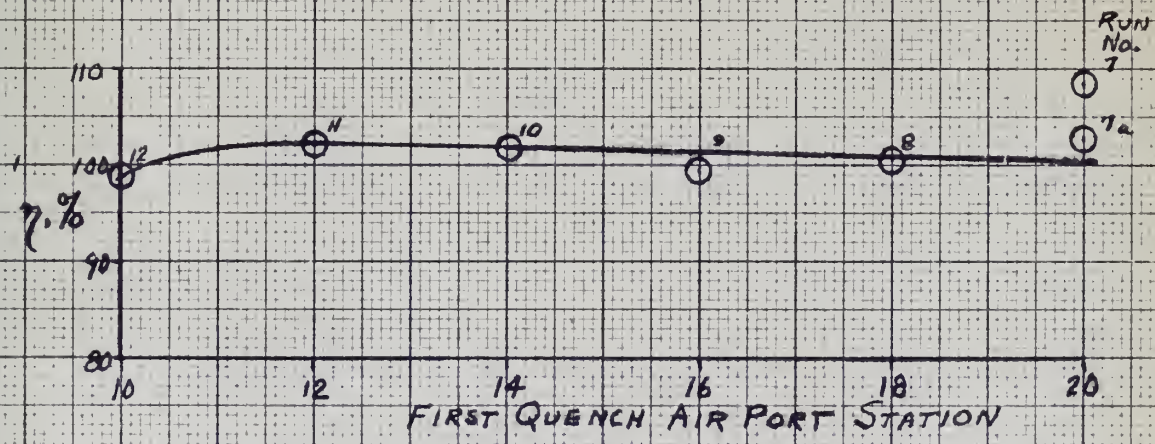

FIGURE 18 - EFFICIENCY AND VELOCITY AND TEMPERATURE EXIT PROFILES VS. QUENCH AIR POSITION, AVIATION GASOLINE.

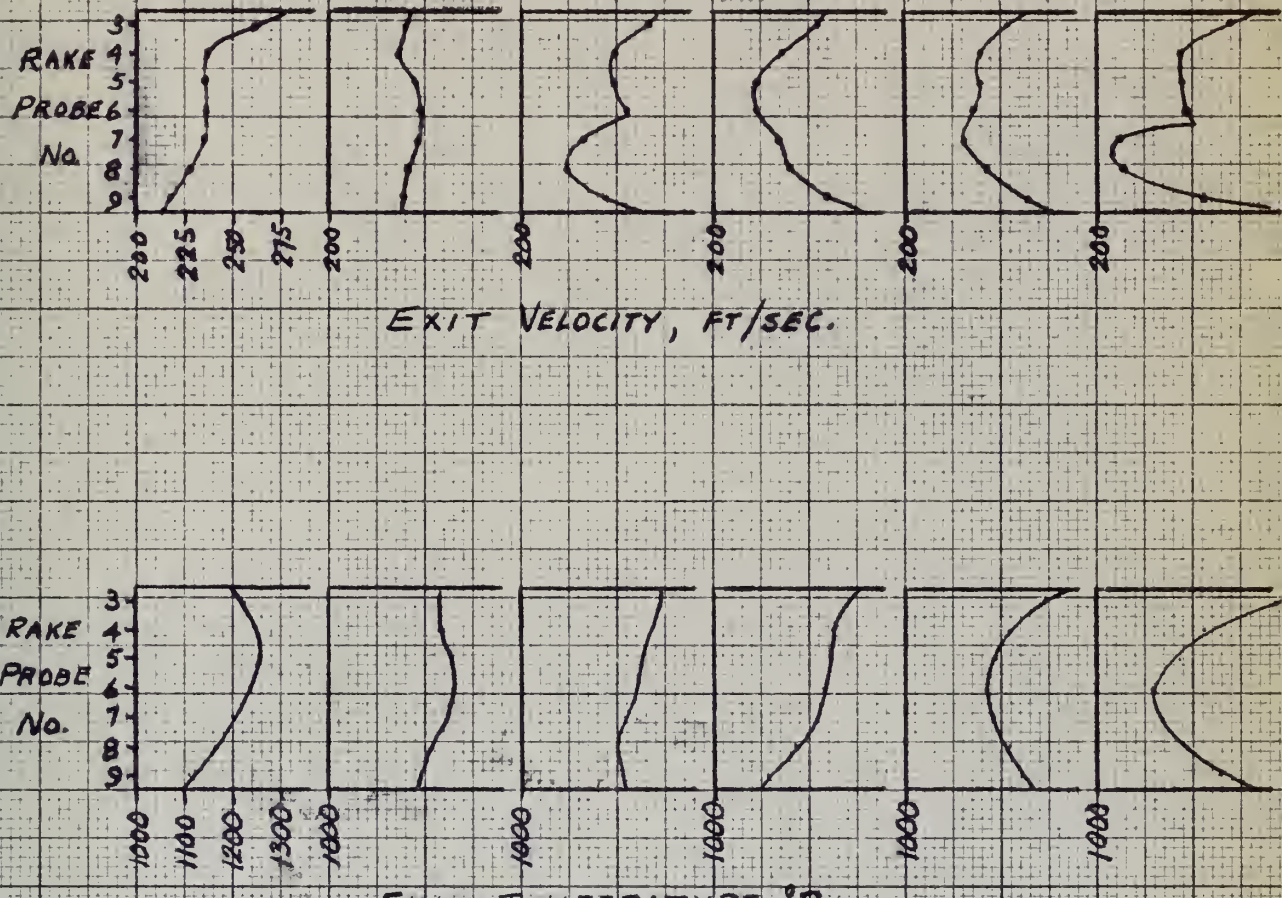

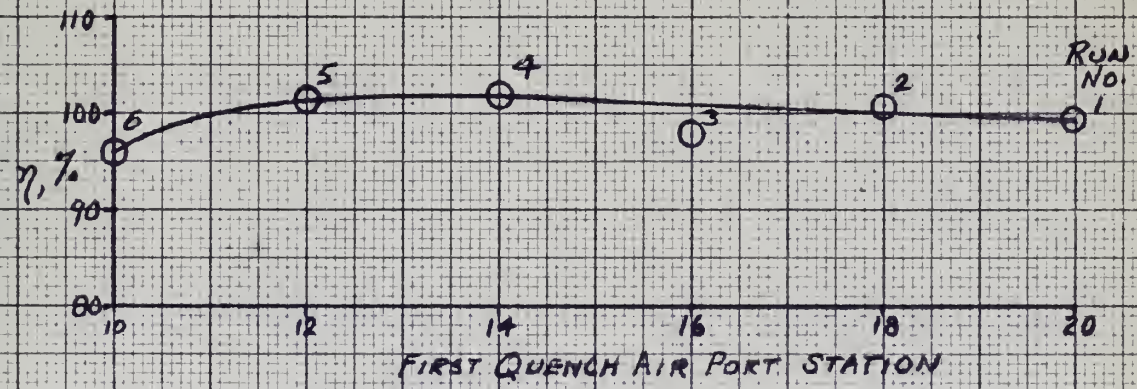

FIGURE 19 - EFFICIENCY AND VELOCITY AND TEMPERATURE EXIT PROFILES VS. QUENCH AIR POSITION, NAPHTHA

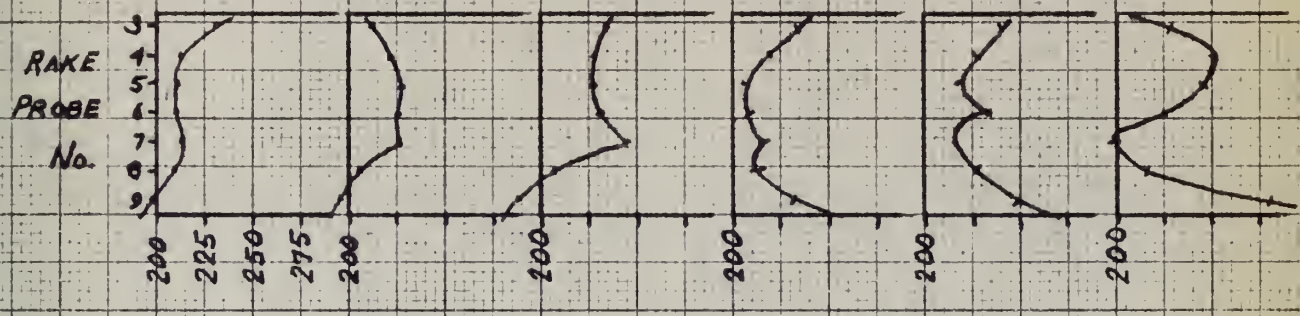

EXIT VELOCITY, FT/SEC.

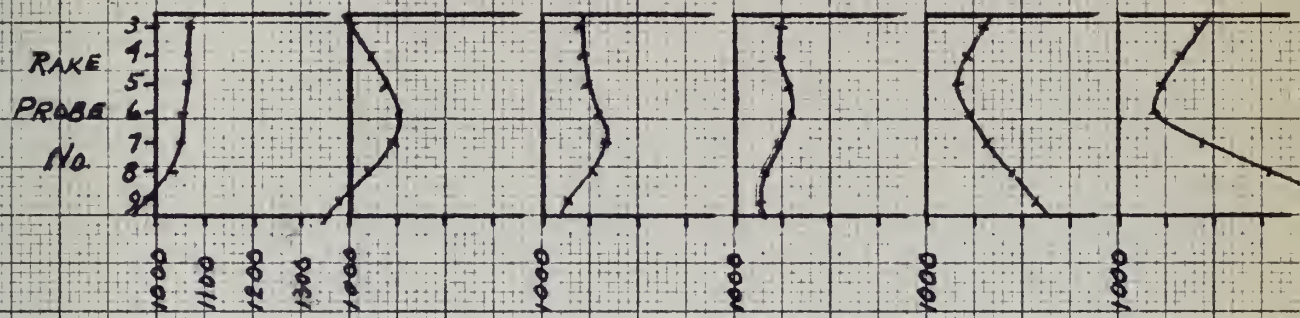

EXIT TEMPERATURE, °R.

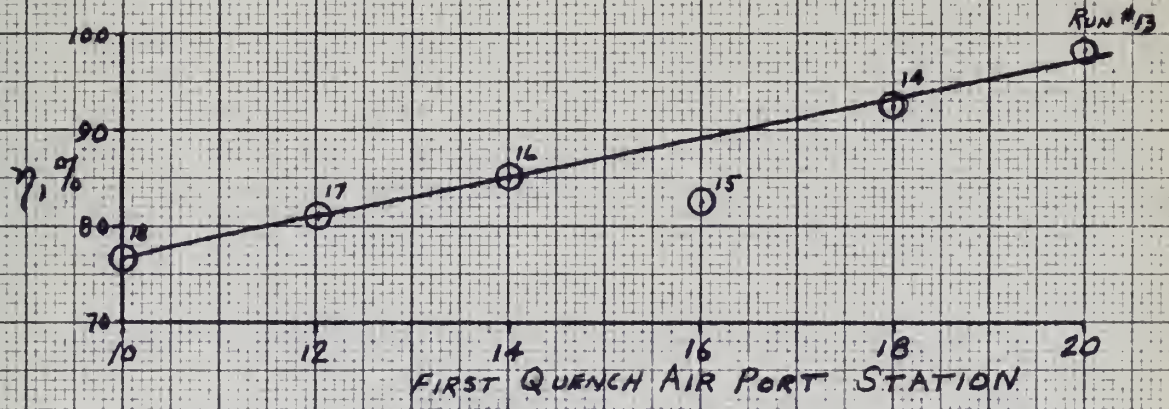

FIGURE 20 - EFFICIENCY AND VELOCITY AND TEMPERATURE EXIT PROFILES VS. QUENCH AIR POSITION, KEROSENE.

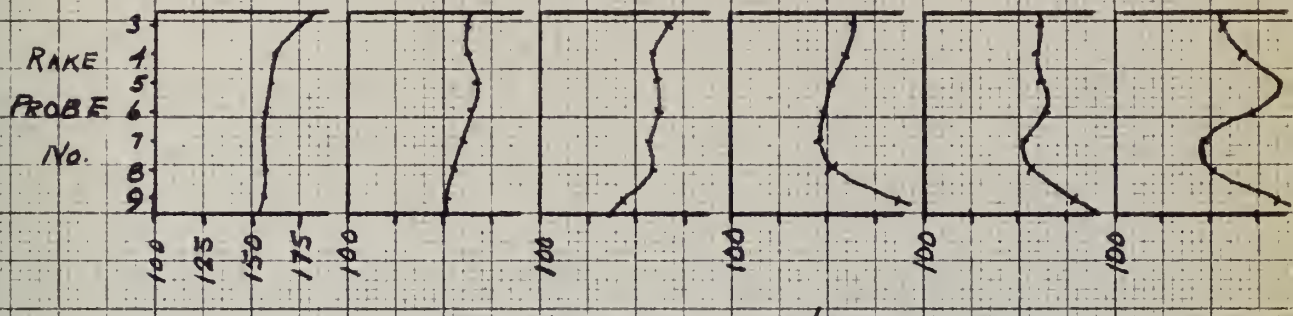

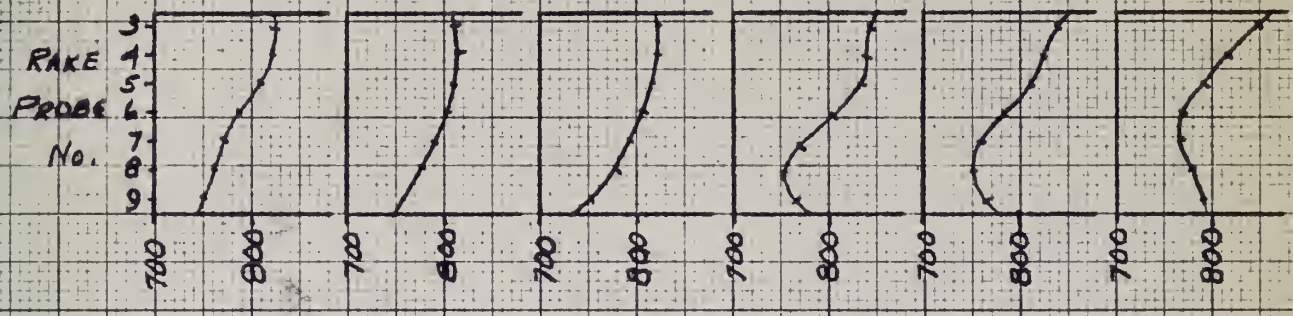

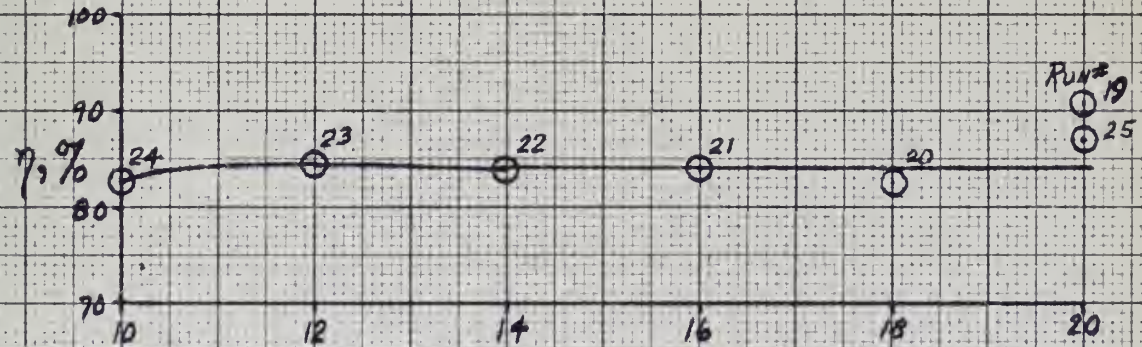

FIGURE 21 - EFFICIENCY AND VELOCITY AND TEMPERATURE EXIT PROFILES VS. QUENCH AIR POSITION, DIESEL FUEL (REDUCED FLOW RATE).

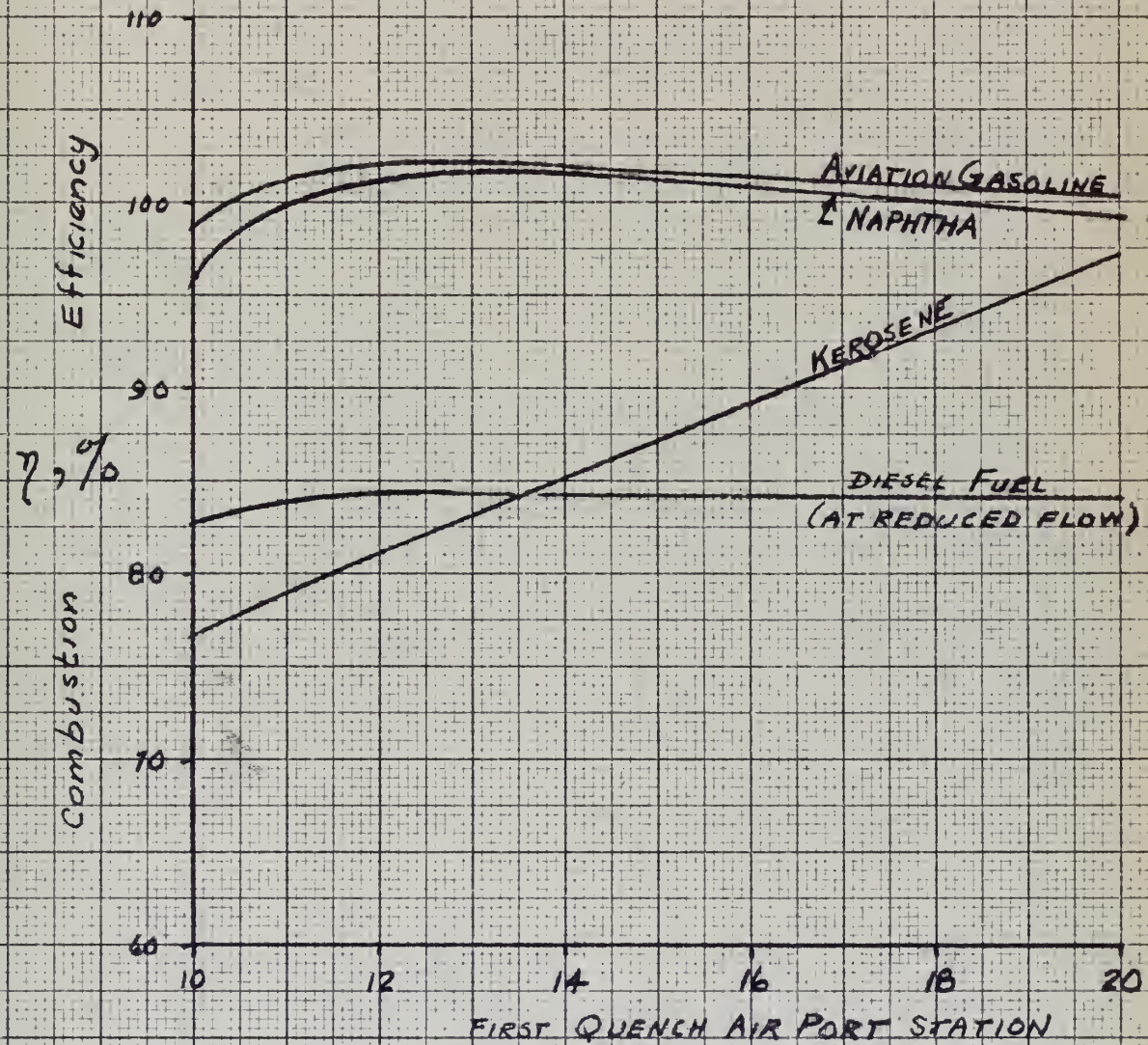

FIGURE 22 - COMPARISON OF EFFICIENCY VS. QUENCH AIR POSITION FOR FOUR FUELS.

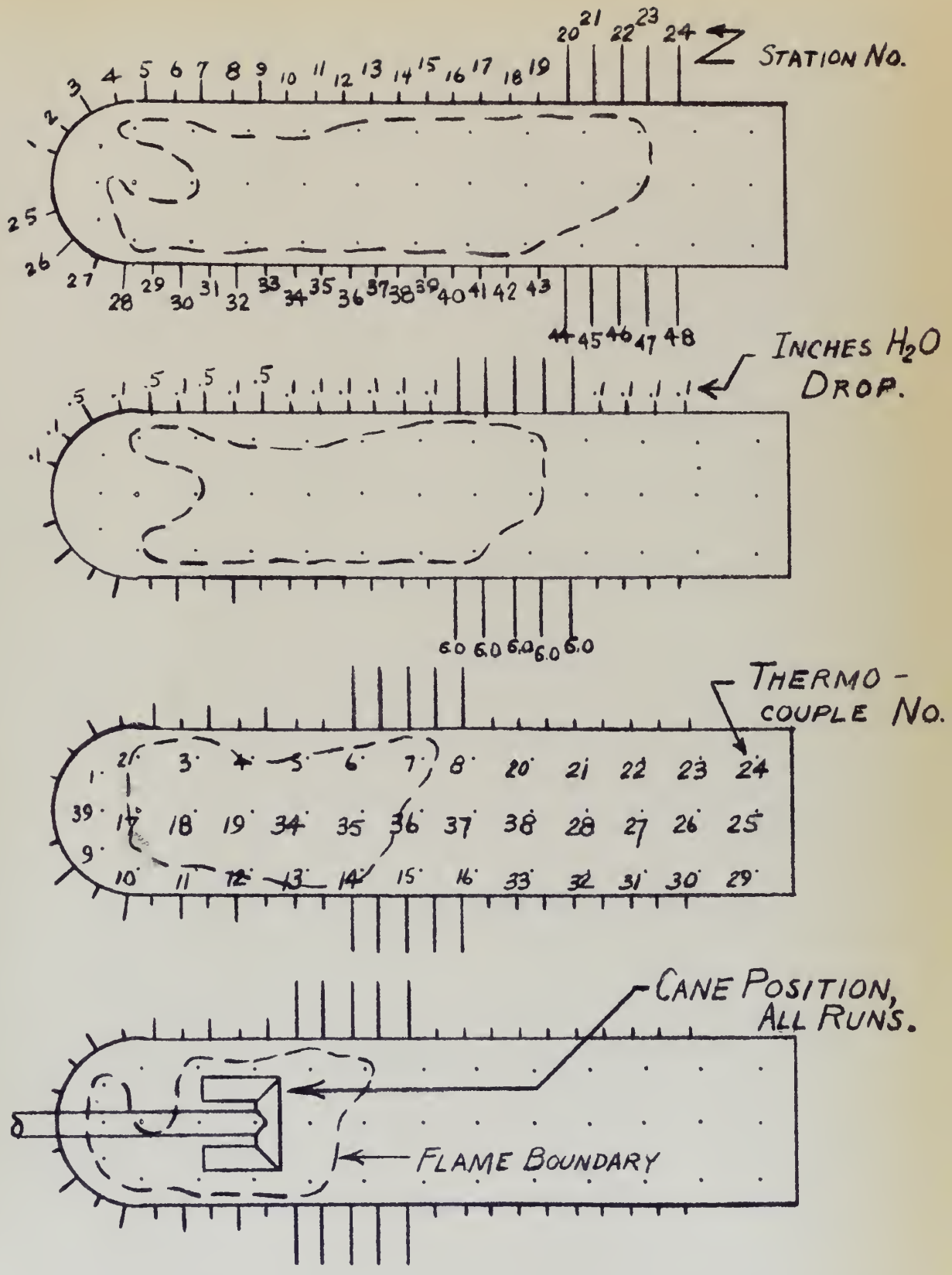

FIGURE 23. FLAME PATTERNS; FUEL, NAPHTHA.

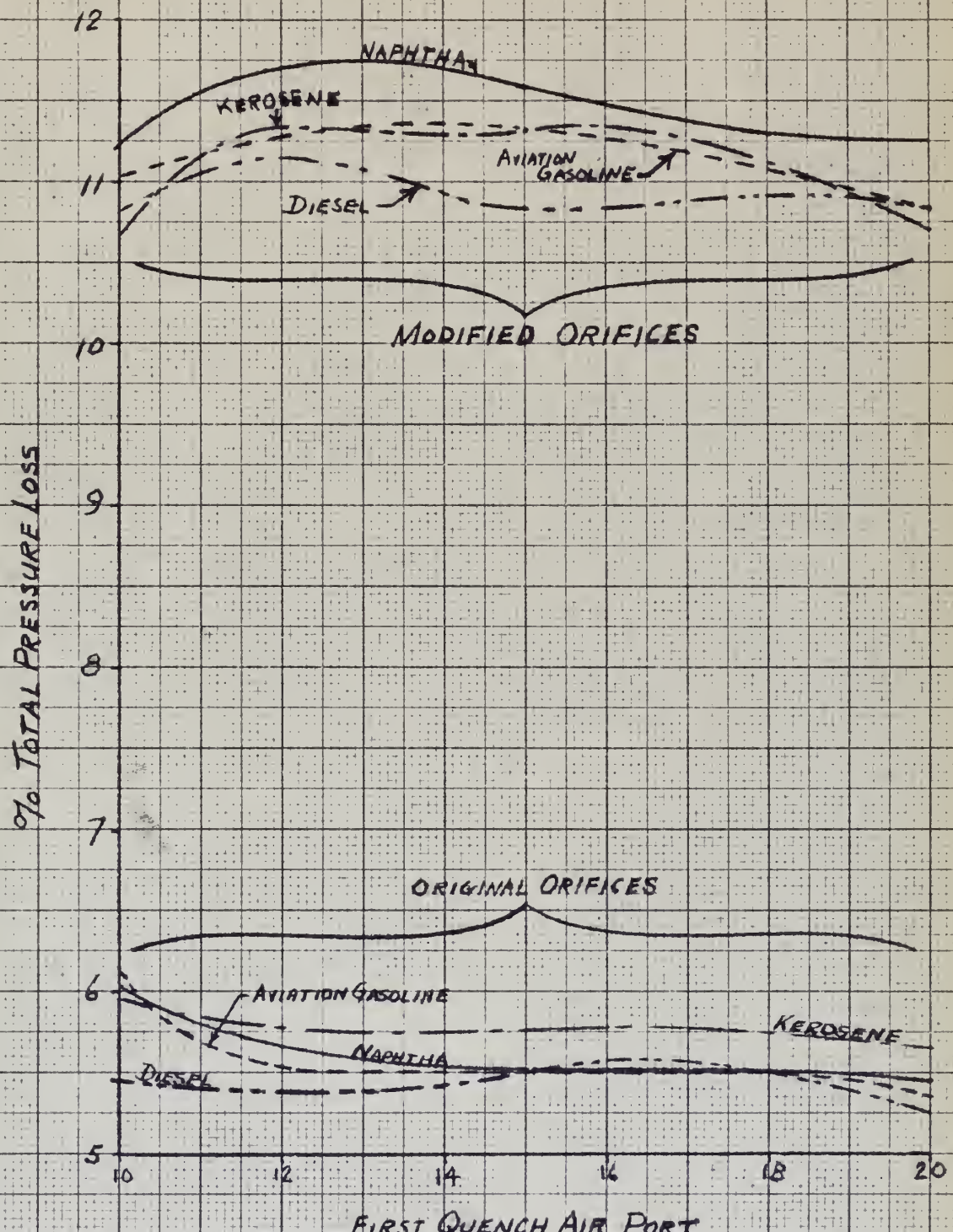

FIGURE 24 - INCREASE IN TOTAL PRESSURE LOSSES DUE TO ORIFICE MODIFICATION AND RESULTANT FLOW.

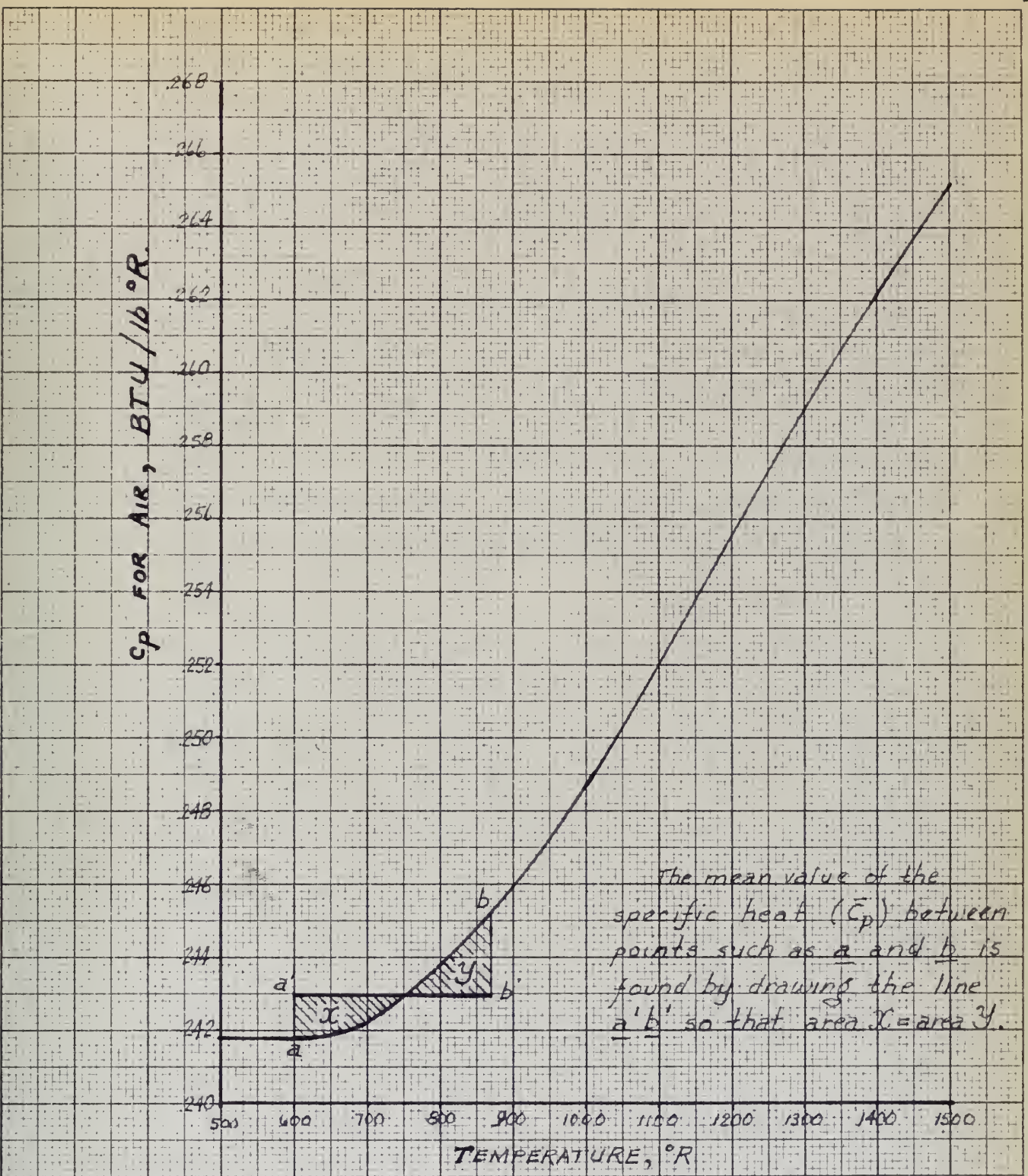

FIGURE 25 - DETERMINATION OF $\bar{c}_p$.

APPENDIX A

FUEL SPECIFICATIONS[6]

The four fuels used in this investigation are the same as those used in the report by J. Ryberg.[7] Although the values of the specific gravity of a particular fuel as used in each investigation differed somewhat, the overall heating value and specific heats did not vary enough to introduce errors for purposes of comparison.

The heating value, latent heat of vaporization, and the weight per cent of hydrogen and carbon were computed from an equation using the specific gravity.[12] As these values did not vary appreciably from the various handbook values, they were accepted as being sufficiently accurate for purposes of calculations in this investigation. The equations used are:

(1) net heating value in BTU/lb = $19960 - 3{,}780 \times (\text{spgr})^2 - 1362 \times (\text{spgr})$. (for const. press.)

(2) latent heat of vaporization in BTU/lb

$$= \frac{110.9 - 0.09 \times \text{temp.}^{\circ}\text{F}}{\text{sp gr}}$$

where $t^{\circ}F$ was chosen as an average between the boiling point and the temp. of the incoming air.

(3) weight % of Hydrogen = $26 - (15 \times \text{spgr})$

(4) weight % of carbon = 100 - wt. % of hydrogen

The specific heats of the fuels were based on equations wherein a factor K[13] was used. This factor is a direct indication

of the fuel characteristics as shown by the equation $K = \frac{\sqrt[3]{T_{bp \text{ in } {}^\circ R}}}{\text{sp gr at } 60^\circ F.}$ It is plotted as a parameter in curves of temperature versus c_p. From the equation

$$C_{p_{ave}} = 1/6 \left(c_{p_{t_1}} + 4c_{p_{t_{av}}} + c_{p_{t_2}}\right)$$

the average c_p may be calculated. The upper and lower values of the temperatures of the fuel vapor were taken as 800°F. and 1500°F. ($C_{p_{t_{av}}} = C_p$ from curve at $\frac{t_1 + t_2}{2}$ while $C_{p_{ave}} =$ final $C_{p_{fuel}}$).

The distillation curves shown in Figure 16 were determined according to the specification given by the ASTM Distillation Code.[14]

The vapor pressures of the fuels were determined with a Reid vapor pressure bomb in accordance with the ASTM specifications and standards.[15]

Densities were determined by use of the Westphal balance.

The fuel properties are found in Table I.

TABLE I

FUEL PROPERTIES

Fuel	Aviation Gas	VM&P Naphtha	Kerosene	Diesel Fuel #2
Specific gravity at 60°F.	0.7249	0.7624	0.8272	0.8708
API specific grav. at 60°F.	63.7	53.3	29.5	31.0
Pounds of fuel per gallon	6.032	6.374	6.890	7.251
Reid vapor pressure - psig	6.15	0.62	0.32	0.35
Boiling point from dist. curve - °F.	204	254	430	495
Latent heat of vapor (const. press.) BTU/#	136	126	108	97
Net heating value - BTU/#	18862	18800	18505	18290
Wt % of hydrogen	15.13	15.15	13.6	12.92
Wt % of carbon	84.87	84.85	86.4	87.08
Specific heat - BTU/# °F.	0.520	0.498	0.519	0.607

APPENDIX B

EFFICIENCY CALCULATIONS

Calculation of thermal efficiency, defined as

$\eta = \frac{\Delta T \text{ actual}}{\Delta T \text{ theoretical}}$, for each run was carried out as follows:

Data recorded:

P_2, ΔP_2, T_2, P_3, ΔP_3, T_3, P_{s_e}, P_1, T_f, $(\Delta P)_i$, T_i, Q_L, C_{p_f}, Fuel, Fuel Flowmeter reading, Air Pattern.

Data computed:

ρ_2, ρ_3, ρ_i, V_i (from $P_{s_i} + \frac{1}{2}\rho_i V_i^2 = P_{T_i}$).

Data obtained from calibration curves:

$\dot{m}_2$, $\dot{m}_3$, $\dot{m}_f$.

Computation procedure:

Average exit cross-section temperature:

$$\frac{\sum \rho_i V_i T_i}{\sum \rho_i V_i} = T_{ave}.$$

Actual temperature rise in burner:

$$T_{act} = T_{ave} - \frac{(\rho_2 V_2 T_2 + \rho_2 V_3 T_3)}{(\rho_2 V_2 + \rho_3 V_3)} = T_{ave} - (T_2 - 1^\circ)$$

Total Mass flow at exit cross section:

$$\dot{m}_m = \sum \rho_i V_i A_i = \sum \rho_i V_i \left(\frac{1}{7}\right)\left(\frac{2.25 \times 5}{144}\right) = 0.01116 \sum \rho_i V_i, \frac{lb}{sec.}$$

Air mass flow at exit cross section:

$$\dot{m}_{air} = \dot{m}_m - \dot{m}_f, \frac{lb}{sec.}$$

$\bar{C}_{p_{air}}$ determined from Fig. 25.

$$C_{p_{mixture}} = \frac{\dot{m}_f C_{p_f} + \dot{m}_{air} \bar{C}_{p_{air}}}{\dot{m}_m}, \frac{BTU}{lb.\,^oR.}$$

Theoretical temperature rise:

$$\Delta T_{theoretical} = \frac{\dot{m}_f Q_L}{(C_{p_{mixture}})(\dot{m}_m)}, \,^oR.$$

$$(= \frac{\Delta T_{actual}}{\Delta T_{theoretical}} \times 100, \%.$$

APPENDIX C

PRESSURE LOSS COMPUTATIONS

Data Recorded:

$$P_2, \Delta P_2, T_2, P_3, \Delta P_3, T_3, P_{s_e}, P_1, (\Delta P)_i, \text{ and } T_i,$$

as defined in SYMBOLS.

Data computed or taken from calibration curves:

$$\rho_2, \rho_3, \dot{m}_2, \dot{m}_3 \text{ and } \rho_i \text{ as defined in SYMBOLS.}$$

Assumption: Velocity profiles upstream of metering orifices are constant.

Formulas used:

(1) $\dot{m} = \rho VA$, lb/sec.

(2) $P_T = P_{total} = P_{static} + \frac{1}{2}\rho V^2$.

(3) $$P_{total} = \frac{\sum P_{total_j} \dot{m}_j}{\sum \dot{m}_j} = \frac{\sum P_{total_j} \rho_j V_j A_j}{\sum \rho_j V_j A_j}$$

Sample calculation (Run #3):

$$P_{T_2} \dot{m}_2 = (P_2 + \tfrac{1}{2}\rho_2 V_2^2)\dot{m}_2 = \left[P_2 + \tfrac{1}{2}\rho_2 \left(\frac{\dot{m}_2}{\rho_2 A_2}\right)^2\right]\dot{m}_2 =$$

$$= \dot{m}_2 P_2 + \frac{\dot{m}_2^3}{2\rho_2 A_2^2}$$

$$= (.5910)(32.55) + \frac{(.5910)^3 (29.92)}{2(.0750)(32.2)(2116)(.1962)^2}$$

$$= 19.378$$

$$P_{T_3} \dot{m}_3 = \dot{m}_3 P_3 + \frac{\dot{m}_3^3}{2\rho_3 A_3^2} = \frac{(.0214)^3(29.92)}{2(.0750)(32.2)(2116)(.1962)^2}$$

$$+ (.0214)(32.17)$$

$$= 0.688 + 0.00000224 = 0.688.$$

Inlet total pressure $= \dfrac{P_{T_2}\dot{m}_2 + P_{T_3}\dot{m}_3}{\dot{m}_2 + \dot{m}_3}$

$$P_{T_{INLET}} = \frac{19.378 + 0.688}{.6124} = 32.80\text{" Hg.}$$

Exit Total Pressure:

$$P_{T_{exit}} = \frac{\sum m_i P_{T_i}}{\sum m_i} = \frac{\sum \rho_i V_i P_{T_i}}{\sum \rho_i V_i}$$

$$= \frac{\sum \rho_i V_i (P_{ambient} + \Delta P_{static} + \Delta P_{impact_i})}{\sum \rho_i V_i}$$

$$= P_{ambient} + \frac{\sum \rho_i V_i (\Delta P_{static} + \Delta P_{impact_i})}{\sum \rho_i V_i}$$

$$= 28.87 + \frac{8.754}{52.48}$$

$$= 28.87 + 0.167 = 29.04\text{" Hg.}$$

Total Pressure Loss:

$$\% P_T \text{ loss} = \frac{P_{T_{inlet}} - P_{T_{exit}}}{P_{T_{inlet}}}$$

$$= \frac{32.80 - 29.04}{32.80} \times 100 = 11.48\%$$

From Ref. 1, the equation for momentum pressure loss in a combustion chamber of variable cross section is

$$\frac{\Delta P}{P_3} = \frac{kM_3^2}{2}\left[\frac{T_4 A_3}{T_3 A_4} - 1\right]$$

where M_3 = inlet Mach number
P_3 = inlet total pressure
A_3 = inlet cross section area
T_3 = inlet cross section temperature
$()_4$ = refers to exit cross-section

To determine the increase in friction pressure loss between those runs by Barnes[6] and those of this investigation the following procedure was used. The total pressure loss for each run in this investigation and for each run which plotted on or near final curves of Barnes[6] was computed in accordance with the procedure previously outlined. Data from runs at high efficiencies (large T_4) are herewith compared. From Run #4 of this investigation, using only main air supply data:

$T_3 = 577^\circ R.$ $\quad \dot{m}_3 = .5910$ lb/sec.

$T_4 = 1241^\circ R.$ $\quad \rho_3 = .0750$ lb/ft^3

$\frac{A_3}{A_4} = \frac{9}{11.25} = 2.510$ $\quad \%P_{T_{loss}} = 11.70\%$

$$M_3 = \frac{V_3}{a_3} = \frac{\dot{m}_3}{\rho_3 A_3 \sqrt{\gamma g R T_3}} = 0.0350$$

$$\frac{\Delta P}{P_3} = \frac{k(.0350)^2}{2}\left[\frac{1241}{577} \times 2.510 - 1\right]$$

$$= k(.000612)\left[5.40 - 1\right] = 0.00257\ k$$

From Run #47 of Barnes:[6]

$T_3 = 546^\circ R.$ $\quad \dot{m}_3 = 0.5980$ lb/sec.

$T_4 = 1167^\circ R.$ $\quad \rho_3 = 0.0749$ lb/ft^3

$\frac{A_3}{A_4} = 2.510$ $\quad \%P_{T_{loss}} = 5.51\%$

$$M_3 = \frac{V_3}{a_3} = \frac{\dot{m}_3}{\rho_3 A_3 \sqrt{\gamma g R T_3}} = 0.0354$$

$$\frac{\Delta P}{P_3} = \frac{k M_3^2}{2}\left[\frac{T_4}{T_3}\frac{A_3}{A_4} - 1\right]$$

$$= k(.0354)^2\left[\frac{1167}{546} \times 2.510 - 1\right] = .00626(4.35)k$$

$$= 0.00272\ k.$$

% change in momentum pressure loss, based on that of Barnes[6] is:

$$\% \text{ change} = \frac{0.00272\,k - 0.00257\,k}{0.00272\,k} \times 100 = 5.52\% \text{ (decrease)}$$

To determine the momentum pressure loss, since the factor "k" is unknown, the relationship that friction pressure loss is of the order of twice the momentum pressure loss[1] is used, yielding, for Barnes'[6] Run #47:

$$\% \text{ Momentum pressure loss} = \frac{1}{3}(5.51)\% = 1.83\%$$

Applying the 5.52% decrease computed above, the momentum pressure loss for Run #4 is 1.73%. This difference of 0.10% (= 1.83% - 1.73%) is insignificant when compared to the total pressure loss (= 11.70%). Therefore, the increase of friction pressure losses between the two investigations has been taken as the difference in the total pressure losses.